4

Fracture Behaviour of Controlled-Rheology Polypropylenes

Alicia Salazar and Jesús Rodríguez
Department of Mechanical Technology,
School of Experimental Sciences and Technology,
University of Rey Juan Carlos, Madrid,
Spain

1. Introduction

The combination of economy, unique properties and ease of recycling offered by polypropylene (PP) leads to its widespread use as a commodity in the food and medical packing, automobile, furniture and toy industries (Karger-Kocsis, 1995; Pasquini, 2005). Some of these applications put stringent demands on PP properties to achieve the final commercial end-uses. PP produced in conventional reactors by fourth generation Ziegler Natta catalyst system presents relatively high molecular weight (M_w) and broad molecular weight distribution (MWD). These features cause high melt viscosity which makes them unsuitable for commercial end-uses such as fiber spinning, blown film and extruded and injection-molded thin-walled products.

The MWD largely determines the rheological properties of polypropylene melts and many physical properties. Therefore, this parameter must be controlled to improve the material response during processing and to achieve the diversity in polymer grades suitable for the different applications of polypropylene. Control of MWD of PP can be done in the conventional reactor through improvement in the polymerization technology or via a post-reactor operation in the original PP with high M_w and broad MWD by means of different degradation methods. The former is not profitable because it requires the addition of chain terminators and transfer agents which normally leads to decrease the output and increase the cost. Instead, the latter technique, such as reactive extrusion, consists of incorporating peroxides to induce controllable degradation of PP chains which efficiently results in polymers with tailor made properties. The polypropylenes prepared this way are termed "Controlled-Rheology Polypropylenes" (CRPP) and they have superior processing properties due to reduced M_w and narrowing MWD (Asteasuain et al., 2003; Azizi & Ghasemi, 2004; Azizi et al., 2008; Baik & Tzoganakis, 1998; Barakos et al., 1996; Berzin et al., 2001; Blancas & Vargas, 2001; Braun et al., 1998; Do et al., 1996; Gahleitner et al., 1995, 1996; Graebling et al., 1997; Pabedinkas et al., 1989; Ryu et al., 1991a, 1991b; Tzoganakis et al., 1989; Yu et al., 1990). The advantages of CRPPs versus reactor made PPs are less shear sensitivity, high elongation at break and heat distortion temperature, surface smoothness and better physical properties such as clarity and gloss (Pabedinkas et al., 1989; Baik & Tzoganakis, 1998). Moreover, the method of reactive extrusion is a simply operation with low cost and high productivity.

The main drawback of PP is its low fracture toughness, especially at low temperatures and/or high strain rates (Hodgkinson et al., 1983; Prabhat & Donovan, 1985). For that reason, a dispersed rubbery phase is incorporated in PP matrix inducing the appearance of toughening mechanisms via either physical blending or by copolymerization with other polyolefins with lower Tg than PP, such as the polyethylene, PE (Karger-Kocsis, 1995; Pasquini, 2005). The copolymerization with ethylene is preferable instead of blend systems due to the strong incompatible nature of polyethylenes and polypropylenes (Teh et al., 1994). The resulting block copolymers are heterophasic materials with a two phase structure where an elastomeric phase in form of spherical domains, usually ethylene-propylene copolymer rubber (EPR), is dispersed uniformly within the PP homopolymer matrix (Sun & Yu, 1991; Sun et al., 1991). As PP homopolymers, these ethylene-propylene block copolymers, EPBCs, also termed as Heterophasic Copolymers (HECO), can be also peroxide degraded to attain different grades. With controlled-rheology (CR) grades of copolymer the M_w is not only reduced by chain cleavage but the ethylene containing block of the copolymer also experiences chain growth. This can lead to a very small decrease in impact strength but the improved flow properties counteract this.

Reactor-made PPs and EPBCs are semicrystalline polymers which have been extensively investigated. The mechanical and fracture response of PPs produced via catalyzers is strongly influenced by the microstructure. There are many reports on the effect of crystallinity degree, size, distribution and shape of spherulites, the lamellar thickness and the crystalline orientation of reactor-made PPs (Allen & Bevington, 1989; Avella et al., 1993; Chen et al., 2002; Dasari et al, 2003b, 2003b; Fukuhara, 1999; Grein et al., 2002; Ibhadon, 1998; Ogawa, 1992; Pasquini, 2005; Sugimoto et al., 1995; Tjong et al., 1995; Van der Wal et al., 1998) and the ethylene content in case of EPBCs (Chen et al., 2002; Doshev et al., 2005; Fukuhara, 1999; Grein et al., 2002; Grellmann et al., 2001; Kim et al. 1996; Lapique et al., 2000; Starke et al., 1998; Sun & Yu, 1991; Van der Wal et al., 1999; Yokoyama & Riccò, 1998) on the mechanical properties.

In case of PP, crazes are the main mechanism of deformation and failure. They are formed in the weak points of the microstructure, normally nearby the intercrystalline regions. Craze structure and extension are closely related to the molecular weight. Several authors have proven that the crack initiation and growth, as well as the breakdrown, are controlled by the amorphous interconnections among the spherulites, the entanglement density of which improves as the molecular weight increases (Allen & Bevington, 1989; Azizi, 2004; Dasari et al, 2003a, 2003c; Fukuhara, 1999; Ibhadon, 1998; Sugimoto et al., 1995; Yokoyama & Riccò, 1998). Gahleitner et al., 1995, 1996, Xu et al., 2001, 2002, and Yu et al., 2003 have also shown that the impact strength is increased for polymers with small spherulite size and low crystallinity.

Failure in EPBCs is related to the dispersed elastomeric particles. Upon loading, small cavities are nucleated at the weak points of the copolymer such as the boundary between the EPR particles and the PP matrix or the intercrystalline zones in the PP matrix (Dasari et al., 200a; Grellmann et al., 2001; Starke et al., 1998; Van der Wal et al., 1999; Yokoyama & Riccò, 1998). These voids are stabilised by fibrillar bridges of PP filaments which are plastically deformed and orientated. As in case of PPs, these fibrillar bridges are stronger as the molecular weight is higher (Fukuhara, 1999; Ibhadon, 1998; Kim et al. 1996; Van der Wal et al., 1999; Yokoyama & Riccò, 1998).

Design engineers need fracture parameters for the construction of structural elements made of PPs and EPBCs in many technological and industrial applications. Although extensive research exists into the reactive mechanism, the rheological and crystallization behaviour as well as the mechanical properties of CRPPs (Asteasuain et al., 2003; Azizi & Ghasemi, 2004; Azizi et al., 2008; Baik & Tzoganakis 1998; Barakos et al., 1996; Berzin et al., 2001; Blancas & Vargas, 2001; Gahleitner et al., 1995, 1996; Pabedinkas et al., 1989; Ryu et al., 1991; Tzoganakis et al., 1989; Yu et al., 1990) and blends of PP and PE (Braun et al., 1998; Do et al., 1996; Graebling et al., 1997; Yu et al., 1990), there is little information on the fracture behaviour of peroxide degraded PP and EPBCs (Sheng et al., 2008) and even less concerned with the influence of supramolecular characteristics as the spherulite size and distribution on the fracture parameters of these materials. In Sheng et al., 2008, the effect on the fracture behaviour with the Post-Yield Fracture Mechanics approach was analyzed through the evaluation of essential work of fracture parameters of controlled-rheology EPBC films. The molecular weight of which was adjusted by reactive extrusion with the incorporation of dicumylperoxide. The results revealed the same tendency as in the case of reactor-made PPs or EPBCs with the same ethylene content but different molecular weight: the fracture toughness decreases as the molecular weight decreases as a result of the addition of peroxide. In addition, there are no explicit researches which tackle with the influence of the spherulite size and distribution on the fracture mechanics parameters of CRPPs, which allow us to extrapolate the results attained in reactor-made PPs (Allen & Bevington, 1989; Avella et al., 1993; Chen et al., 2002; Dasari et al., 2003a, 2003b; Fukuhara, 1999; Ibhadon, 1998; Van der Wal et al., 1998; Xu et al., 2001, 2002; Yu et al., 2002). Even more, most of the results found in the literature have been performed on thermally treated specimens with controlled spherulitic architectures and sizes (Avella et al., 1993; Chen et al., 2002; Dasari et al., 2003a, 2003b, 2003c; Gahleitner et al., 1995, 1996; Ibhadon, 1998; Wang et al., 2008; Xu et al., 2001, 2002; Yu et al., 2002) but not on real injected or extruded samples, ready for engineering or industrial applications.

For all those reason, the present chapter is focussed on:

1. Analyzing the evolution of the fracture toughness parameters of different grades of PP homopolymer and EPBCs prepared controlling the addition of peroxide in reactive extrusion. The fracture strength of these CRPPs and controlled-rheology EPBCs is determined through J-integral methodologies, paying special attention to the analysis of the micromechanisms of failure via optical microscopy and scanning electron microscopy. An analysis of the rheological, thermal and mechanical response is also provided.
2. Discussing the effect of the peroxide content, the structural parameters (MW, MWD) and the supramolecular characteristics such as the spherulite size and distribution on the fracture toughness parameters and the failure mechanisms. The analysis is carried out on real injected CRPPs in which neither thermal treatment was applied nor nucleating agents were used.
3. Evaluating the goals and limitations of controlled-rheology grades over conventional ones through the analysis of the fracture toughness parameters. For that, a controlled-rheology EPBC and a reactor-made EPBC with similar structural properties were examined.

2. Methodologies for the fracture characterization

In many in-service applications, PPs and EPBCs present a pronounced non linear mechanical response brought about by contained plastic deformation. Elastic-Plastic Fracture Mechanics (EPFM) approach through the J-integral methodologies is to be used to achieve the fracture toughness at crack initiation, J_{IC}, which is determined from the crack resistance curve, J-R curve, where J is plotted versus the crack extension, Δa. For the J-R curves construction of polymers, ESIS (Hale & Ramsteiner, 2001) and ASTM D6068 recommend the multiple specimen method. This methodology, though straightforward and effective, is time and material intensive, as at least a minimum of seven specimens have to be tested to generate the R-curve. For that reason, indirect methods have been developed to obtain J-R curves with fewer specimens and, thus, less time requirements. The single specimen methods are based on the load separation criterion (Ernst et al., 1981), and offer an easy and effective alternative approach to obtain J-R curves. Among the single specimen methods, the normalization method (Baldi & Riccò, 2005; Bernal et al., 1996; Landes and Zhou, 1993; Morhain & Velasco, 2001; Rodríguez et al., 2009; Varadarajan et al., 2008) and the load separation parameter method have been successfully applied to polymeric materials (Rodríguez et al., 2009; Salazar & Rodríguez, 2008; Wainstein et al., 2007). Next, a brief description of the methods utilized is presented.

2.1 Multiple specimen method

The multiple specimen method, first proposed by Landes and Begley, 1974, is the most common approach for deducing J-R curves. The basic guidelines of ESIS TC4 Protocol "J-Fracture toughness of polymers at slow speed" are applied (Hale & Ramsteiner, 2001). A set of identical specimens is loaded to various displacements, unloaded, cooled at low temperatures and finally fractured. The initial and final stable crack lengths are measured physically from the broken surfaces, while J is calculated from the total energy required to extend the crack, U, which is determined from the area under the load versus load-point displacement curve up to the line of constant displacement corresponding to the termination of the test:

$$J = \frac{2U}{B(W - a_0)} \tag{1}$$

where B is the specimen thickness, W is the specimen width and a_0 is the initial crack length.

2.2 Normalization method

The J-R curves obtained via the normalization method is focussed on determining accurate crack length predictions using the load (P)-displacement (δ) data alone. The instructions given by ASTM E1820-06 were taken as a guide. Although this test method covers the procedures for the determination of fracture toughness of metallic materials, it has proven its applicability to polymeric materials (Baldi & Riccò, 2005; Bernal et al., 1996; Landes and Zhou, 1993; Morhain & Velasco, 2001; Rodríguez et al., 2009; Varadarajan et al., 2008).

The first step for the determination of the J-R curve is an optical crack-length measurement of the initial, a_o, and final, a_f, crack lengths. Subsequently, each value of the load P_i up to, but not including P_{max} is normalized using the following expression:

$$P_{Ni} = \frac{P_i}{WB\left[\frac{W - a_{bi}}{W}\right]^{\eta_{pl}}} \tag{2}$$

with η_{pl} = 2 for three point bending specimens (SENB). a_{bi} is the blunting corrected crack length given by:

$$a_{bi} = a_o + \frac{J_i}{2m\sigma_{ys}} \tag{3}$$

$$J_i = \frac{K_i^2\left(1-\nu^2\right)}{E} + J_{pli} \tag{4}$$

where σ_{ys} is the yield stress and m is a dimensionless constant that depends on stress state and materials properties, named as crack tip constraint factor. m=1 has been reported for PP based materials (Morhain & Velasco, 2001; Rodríguez et al., 2009). In turn, K_i is the stress intensity factor, E is the Young´s modulus, ν is the Poisson´s ratio and J_{pl} is the plastic part of the J-integral according to ASTM E1820-06.

Each corresponding load line displacement, δ_i, is normalized to give a normalized plastic displacement:

$$\delta'_{pli} = \frac{\delta_{pli}}{W} = \frac{\delta_i - P_i C_i}{W} \tag{5}$$

being C_i the specimen elastic load line compliance, based on the crack length a_{bi}.

Thus, data points up to maximum force are normalized. In order to obtain the final point, the same equations are employed, but instead of the initial crack length, the final crack length is used. The normalized plastic displacement values above 0.001 up to maximum force, excluding P_{max} value itself, and the points obtained with the use of the final crack length are used for the normalization function fit. The normalization function can be analytically expressed:

$$P_N = \frac{a + b\delta'_{pl} + c\delta'^2_{pl}}{d + \delta'_{pl}} \tag{6}$$

where a, b, c and d are searched fitting coefficients. When the fitting parameters are determined, an iterative procedure is further applied to force all P_{Ni} data to lie on the fitted curve by ai adjustment. Knowing P_i, δ_i and a_i values the construction of the J-R curve is followed with J-integral values given by:

$$J = \frac{2U_i}{B(W - a_0)} \tag{7}$$

where U_i is determined from the area under the load versus load-point displacement curve up to (P_i, δ_i); versus $\Delta a_i = a_i - a_o$.

2.3 Determination of the crack growth initiation energy, J_{IC}

Once the J-R curve is constructed either by the multiple specimen or the normalization method, it should be described by a power law $J=C\cdot\Delta a^N$, with $N\leq 1$. The crack initiation resistance or fracture toughness, J_{IC}, is calculated as a pseudo-initiation value $J_{0.2}$, which defines crack resistance at 0.2 mm of the total crack growth (Hale & Ramsteiner, 2001).

The size requirements for plane strain J_{IC} are given by (Williams, 2001):

$$B, a, W-a > 25\frac{J}{\sigma_{ys}} \tag{8}$$

3. Materials and sample preparation

The materials under study were an ISPLEN polypropylene homopolymer, PP0, and two ethylene-propylene block copolymers, EPBC0 and EPBC0-2, with an ethylene content of ~8 wt%, supplied by REPSOL Química. They were manufactured using a Spheripol process with a fourth generation Ziegler-Natta catalyst. The peroxide used was di-tert-butylperoxide (DTBP).

The reactive experiments and sample preparation were carried out using a twin-screw extruder, Werner & Plfeiderer (model ZSK-30), with a length/diameter ratio of the dies, L/D, of 25. In case of PP, the peroxide and the PP0 were premixed to prepare master batches using 0, 154, 402 and 546 ppm of peroxide content. Instead, for the copolymers, the starting reactor-made copolymer for the reactive extrusion experiments was EPBC0. So, the peroxide was added to the EPBC0 to obtain master batches with peroxide contents of 0, 101, 332 and 471 ppm. Independently of the grade, both components were inserted into the extruder. Experiments were performed at a profile temperatures of 190, 220, 240, 220, 200 ºC for the PP and of 190, 220, 240, 220 ºC for the EPBC with a screw rotation speed of 150 rpm in both cases. Extrudates were cooled through a water bath and were granulated. Samples for mechanical and fracture properties were injection moulded.

4. Experimental procedure

4.1 Melt flow rate and molecular weight characterization

Melt flow rate (MFR) was measured following the ISO 1133 standard using a Ceast 6932 extrusion plastometer at 230ºC/2.16 kg.

The molecular weight distributions were determined with Gel Permeation Chromatography (GPC) using a Polymer Labs PL220 equipment and taking ISO 14014 as a guide. The samples were dissolved at 143 ºC in 1,2,4 trichlorobenzene at a polymer concentration of 1.3 mg/ml. A phenolic antioxidant Irganox 1010 was added to the solution to prevent any degradation.

4.2 Thermal analysis

The apparent melting temperature, T_m, the crystallinity temperature, T_c, and the crystallinity index, α, of all the samples were measured via Differencial Scanning Calorimetry (DSC)

using a Mettler-Toledo (model DSC822) equipment. Two scans were done at 10 ^{o}C/min, from 0 to 200 ^{o}C under nitrogen atmosphere, in aluminum spans with 10 mg of sample. The values of T_c were obtained from the maxima of the crystalline peaks meanwhile the values of T_m and the apparent enthalypy, ΔH, were calculated from the maxima and the area of the melting peaks, respectively. The crystallinity index via this technique was determined using

$$\alpha = \frac{\Delta H}{\Delta H^0} \tag{9}$$

where the enthalpy of fusion of 100% pure crystalline α-PP, ΔH^0, was taken as 190 J/g (Pasquini, 2005).

4.3 Supramolecular characterization: Determination of spherulite size

Films with 3 μm in thickness were sectioned from the centre of bulk injected specimens with a microtome (Rotary Microtome Leica RM2265) as the fracture process in the notched specimens occurs within the sample. The films were immersed in a solution containing 1.3 wt% potassium permanganate, 32.9 wt% dry H3PO4 and 65.8 wt% concentrated H2SO4 for 36 h at room temperature (Thomann et al., 1995; Wei et al., 2000). The etched samples were subsequently washed in a mixture of 2 parts by volume of concentrated sulphuric acid and 7 parts of water for 15 minutes in an ultrasonic bath. The resulting sections were picked up and mounted on microscope slides to be analyzed via transmitted light microscopy (Leica DMR) or Au-Pd sputter coated for scanning electron microscopy (Hitachi S-3400N).

Ten scanning views were chosen randomly under enlargement at 1000x for quantitative determination. The image analysis software Image Pro-Plus 4.5 was used to obtain the distribution and spherulite size, taken as the maximum length inside the spherulite. Percentage of porosity was also determined from the microstructural images.

4.4 Mechanical characterization

Tensile tests were carried out, following the ISO527-2:1997 standard, in order to measure the yield stress, the stress at break and the strain at break. Specimens with 10x115x4 mm in the narrow section were tested on an electromechanical testing machine (MTS Alliance RT/5) under displacement control at a cross-head speed of 50 mm/min. Strain values were measured with a high strain extensometer (model MTS DX2000) attached to the sample.

Flexure tests were performed following the guidelines described in ISO178:2003 standard to determine the Young´s modulus. Samples with 10x80x4 mm were tested on an electromechanical testing machine (INSTRON 4465) under stroke control at a cross-head speed of 2 mm/min.

4.5 Fracture characterization

At room temperature and under low loading rates, PPs and EPBCs present a pronounced nonlinear mechanical response. The ESIS TC4 Protocol entitled "The determination of J-fracture toughness of polymers at slow speed" (Hale & Ramsteiner, 2001), was followed to achieve the J-R curves from multiple specimens of CRPPs. In turn, the guidelines given by

ASTM E1820-06 were ensued to achieve via the normalization method the J-integral response of controlled-rheology EPBCs.

Fracture toughness tests were carried out at 23 ºC on single edge notch bending (SENB) specimens obtained directly from the mould with 6x18x79 mm in size and an initial notch length of 8.1 mm. A sharp crack was created by sliding a razor blade into the root of the mechanized notch. The resulting initial crack length was ~ 9.0 mm. Some recent results question the validity of this notch sharpening procedure because some damage can be produced ahead of the crack tip (Salazar et al., 2010a, 2010b, 2010c). Therefore, the fracture toughness obtained from this type of specimens should be considered as an upper limit.

The tests were conducted for each material at room temperature and under displacement control at a cross-head speed of 1 mm/min using a three-point bend fixture of 72 mm loading span. An electromechanical testing machine (MTS Alliance RF/100) with a load cell of ± 5 kN was utilized.

After the tests, the fracture surfaces of the broken specimens were examined using light microscopy (Leica DMR) and scanning electron microscopy (Hitachi S-3400N) to analyze the extension of the stress-whitened region due to plastic deformation as well as the micromechanisms of failure. For scanning electron microscopy analysis, the samples were Au-Pd sputter coated.

5. Results and discussion

5.1 MWD and MFR

5.1.1 Controlled-rheology PPs

Table 1 collets the MFR and the GPC results for the polypropylene with 0, 154, 402 and 546 ppm of peroxide content termed as PP0, PP-CR154, PP-CR402 and PP-CR546, respectively. Several conclusions can be drawn from the analysis of these data. Firstly, MFR increased remarkably with increasing the peroxide content. Secondly, controlled-rheology polypropylene drops more abruptly the weight average molecular weight, M_w, than the number average molecular weight, M_n. As a consequence, the MWD, described by the ratio M_w/M_n, got narrower. The reduction in the MWD reached up to ~ 40% and was in agreement with the decrease observed by other researchers for similar peroxide contents (Baik & Tzoganakis, 1998; Barakos et al., 1996; Berzin et al., 2001; Gahleitner et al., 1995, 1996). Thirdly, the main differences in M_w were found for a small concentration of peroxide, PP-CR154, while there were no pronounced changes among the controlled-rheology polypropylenes. Finally, all these results confirm that increasing the amount of peroxide leads to more chain scission, reducing efficiently the length of the chains.

	MFR (g/10min)	M_w (kg/mol)	M_n (kg/mol)	MWD (M_w/M_n)
PP0	11	319.1	51.7	6.16
PP-CR154	26	238.6	49.5	4.81
PP-CR402	48	179.4	45.6	3.93
PP-CR546	59	172.0	44.0	3.90

Table 1. Melt flow rate (MFR), weight and number average molecular weights (M_w and M_n) and molecular weight distribution (MWD) of the PP, PP-CR154, PP-CR402 and PP-CR546

5.1.2 Controlled-rheology EPBCs

Table 2 summarizes the ethylene content, MFR and the GPC results for the ethylene-propylene block copolymers with 0, 101, 332 and 471 ppm of DTBP content termed as EPBC0, EPBC-CR101, EPBC-CR332 and EPBC-CR471, respectively. As expected, the MFR increased noticeably with increasing the peroxide content, decreasing also the average molecular weights of EPBC-CRs. However, the MWD reduced as much as 30%. This diminish contrasted with those obtained for controlled-rheology polypropylenes homopolymers, which underwent much more degradation for similar peroxide contents (Table 1). Berzin et al., 2001 noted the presence of high residual masses, which indicates the presence of long chains, for the copolymers even for the more degraded products. PP/PE mixtures are known to show opposite effects during peroxide-initiated scission reactions (Berzin et al., 2001; Braun et al., 1998; Do et al., 1996; Graebling et al., 1997). While for the PP matrix, the free radicals formed from the thermal decomposition of the organic peroxide lead to β-scissions because of the low stability of the tertiary hydrogen atoms of macroradicals, for the PE, peroxide attack leads to chain branching and to crosslinking by macroradical recombination. These two competing mechanisms could be the reason for the much lesser reduction in MWD for copolymers than in homopolymers during peroxide degradation.

	Et (wt%)	MFR (g/10min)	M_w (kg/mol)	M_n (kg/mol)	MWD (M_w/M_n)
EPBC0	7.78	12	287.0	56.4	5.09
EPBC0-2	8.62	18	264.1	56.0	4.72
EPBC-CR101	8.19	20	253.0	53.3	4.75
EPBC-CR332	8.36	41	199.4	53.5	3.73
EPBC-CR471	7.91	63	178.2	50.3	3.54

Table 2. Ethylene content (Et), melt flow rate (MFR), weight and number average molecular weights (M_w and M_n) and molecular weight distribution (MWD) of the EBPC0, EPBC0-2, EPBC-CR101, EPBC-CR332 and EBPC-CR471.

This table also shows the basic rheological properties of another reactor-made EPBC, EPBC0-2, with similar characteristics to the peroxide degraded copolymer with the lowest peroxide content, EPBC-CR101.

5.2 Thermal properties

5.2.1 Controlled-rheology PPs

Table 3 shows the apparent melting temperature, T_m, the crystallinity temperature, T_c, the apparent enthalpy, ΔH, and the crystallinity index, α, obtained from DSC measurements for polypropylenes PP0, PP-CR154, PP-CR402 and PP-CR546. All the values measured are in accordance with data reported in the literature (Karger-Kocsis, 1995; Pasquini, 2005). T_m decreased with the peroxide content while T_c and α remained constant. The evolution of T_m with the peroxide content underwent the same trend as that of the M_w with peroxide content among the controlled-rheology polypropylenes (Table 1). However, the present results stood up for the no enhancement of either the crystalline degree or the crystallinity

temperature with the peroxide content. Therefore, the total mass fraction of lamellae must be constant and the major expected difference in structure must be an increase in entanglement density of the amorphous zone with molecular weight attending to the tendency shown by T_m with molecular weight. This behaviour was also reported by Tzoganakis et al., 1989 for polypropylene homopolymers.

	T_m (ºC)	T_c (ºC)	ΔH (J/g)	α (%)
PP0	165	118	112	56
PP-CR154	163	118	104	55
PP-CR402	161	118	104	55
PP-CR546	161	118	104	55

Table 3. Melting temperature, T_m, crystallinity temperature, T_c, apparent enthalpy, ΔH, and crystallinity index, α, obtained from DSC measurements of the polypropylenes PP0, PP-CR154, PP-CR402 and PP-CR546

5.2.2 Controlled-rheology EPBCs

The results of the thermal analysis carried out on EPBCs with different DTBP content are listed in Table 4. As in case of the PP homopolymers, the melting peak temperature reduced with the peroxide content while the crystallization temperature was almost constant. However, the main difference was found in the crystallinity degree, which slightly decreased with the peroxide content. During the degradation of the copolymer, both chain scissions in the PP matrix and crosslinks in the elastomeric phase were produced. Berzin et al., 2001, Braun et al., 1998 and Do et al., 1996 have reported that extensive crosslinks of the elastomeric phase should disturb the crystallinity, reducing not only the size but even the amount. This might be the reason of the slight reduction in the crystalline behaviour of the EPBC-CRs and was confirmed when comparing the crystallinity degree between the reactor made EPBC0-2 and the controlled-rheology EPBC-CR101. Although these reactor-made and controlled-rheology grades presented similar structural properties (Table 2), the reactor-made showed higher crystallinity degree than the peroxide degraded EPBC. This clearly responds to the crosslinking disturbance in the spherulite architecture of the latter.

	T_m (ºC)	T_c (ºC)	ΔH (J/g)	α (%)
EPBC0	164	123	95	53
EPBC0-2	164	118	95	53
EPBC-CR101	164	122	94	51
EPBC-CR332	163	122	93	50
EPBC-CR471	162	123	91	49

Table 4. Melting temperature, T_m, crystallinity temperature, T_c, apparent enthalpy, ΔH, and crystallinity index, α, obtained from DSC measurements of the various EPBCs

5.3 Spherulite size and distribution characterization

The crystal morphology of PP0 and controlled-rheology PPs, PP-CR154, PP-CR402 and PP-CR546, is shown in Figures 1a, 1b, 1c and 1d, respectively. The spherulitic morphology is composed of an aggregate of lamellae that radiate from the centre outward, typical of

monoclinic α-form of isotactic PP, iPP (Karger-Kocsis, 1995; Pasquini, 2005; Thomann et al., 1995). The spherulite size was uneven and it seemed to increase with the addition of peroxide content. Moreover, small pores with ~ 1 μm in diameter are also discernible in those images associated to controlled-rheology polypropylenes with high peroxide content. These pores were originated during the sample manufacture mainly due to poorly residual left peroxide removal as no pores were found in any of the analyzed PP0 images. The percentage of porosity is collected in Table 5. As shown, porosity increased with peroxide content, attaining the highest increase for the materials with 402 and 546 ppm of peroxide.

	Porosity (%)	$\bar{D}$ (μm)	σ^2 (μm^2)
PP0	0	21.8	15.8
PP-CR154	4.8 ± 0.1	27.5	13.7
PP-CR402	7.2 ± 0.2	33.3	7.8
PP-CR546	13.6 ± 1.1	35.2	8.4

Table 5. Porosity and normal distribution parameters of the spherulite size of propylene homopolymer, PP0, and the controlled-rheology-polypropylenes, PP-CRs: mean spherulitic size, $\bar{D}$, and variance, σ^2.

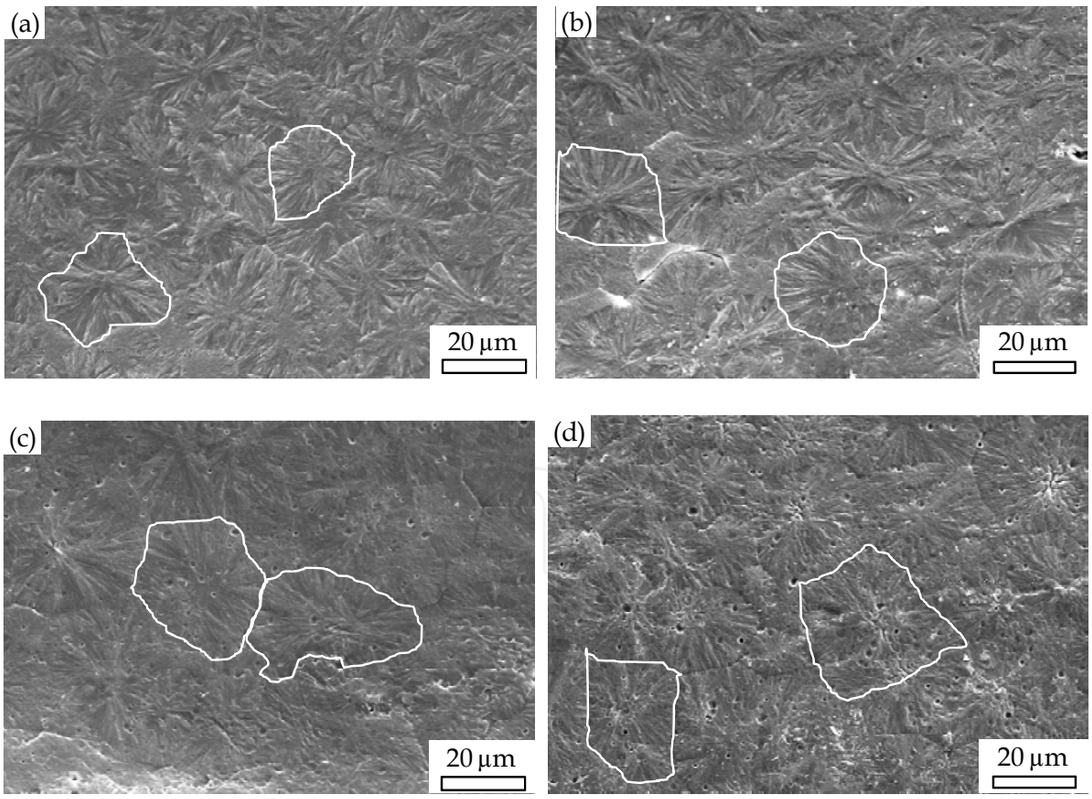

Fig. 1. SEM images at a magnification of x1000 showing the spherulitic mofphology of (a) polypropylene homopolymer, PP0, and controlled-rheology polypropylenes, CRPPs, with (b) 154, (c) 402 and (d) 546 ppm of peroxide content. By way of example some spherulites have been outlined with white lines.

The resulting analysis of the spherulite size led to histograms that were approximated to a normal or Gaussian distribution as the kurtosis for all the materials reached values of utmost 0.15, whereas the perfect Gaussian distribution takes values of 0 (Sheskin, 2000). Thus, the normal distribution in spherulite size for all the materials under study is a number average and are combined in Figure 2, whereas the statistical parameters as the mean spherulitic size, $\bar{D}$, and the variance, σ^2, are collected in Table 5. Firstly, the addition of peroxide increased the spherulite size but not the crystalline percentage (Table 3). The rise in peroxide content drives more chain scission and therefore, reduces efficiently the length of the chains. Although some works are found in the literature reporting the increase in the crystalline fraction as the decrease of chain length promotes more nucleating sites and so easier forming of crystals (Gahleitner et al., 1995, 1996; Azizi & Ghasemi, 2004; Wang et al., 2008), the present results stand up for the no enhancement of the crystalline degree with the peroxide content because the total mass fraction of lamellae maintains constant with the only growth in the spherulite size at the expense of the reduction in the density of tie molecules (Tzoganakis et al., 1989; Ryu et al., 1991). Secondly, the distribution width, represented by σ^2, tended to decrease with the peroxide content. This indicates that the addition of peroxide not only seems to increase the spherulite size but also to a slightly more uniform distribution (Xu et al., 2002).

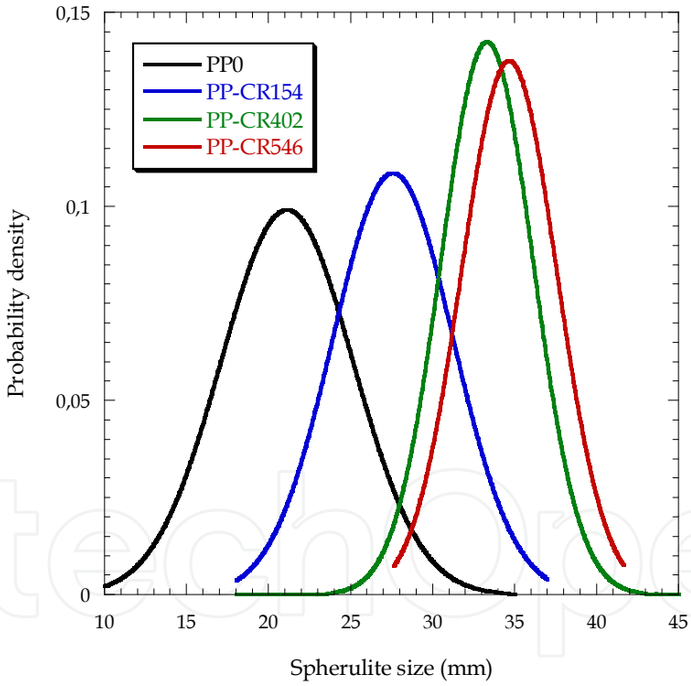

Fig. 2. Normal distributions of the spherulite size for polypropylene homopolymer, PP0, and controlled-rheology polypropylenes, CRPP154, CRPP402 and CRPP546.

5.4 Mechanical characterization

5.4.1 Controlled-rheology PPs

The average Young´s modulus, E, the yield stress, σ_{ys}, the tensile strength, σ_t, and the elongation at break, ε_r, together with their corresponding standard deviations, are

summarized in Table 6. Regarding the elastic properties, the Young´s modulus decreased with the addition of peroxide. The elastic modulus is highly dependent on the amount of stiffest part of the structure, that is, the crystalline region (Avella et al., 1993; Dasari et al., 2003a, 2003c; Gahleitner et al., 1995; Van der Wal et al., 1998). The crystallinity percentage reduced scarcely with a small amount peroxide and held constant for higher additions of peroxide. The evolution of the Young´s modulus with the peroxide content does not correlate with the trend shown by the percentage of crystalline with the peroxide addition. Nevertheless, apart from the crystallinity degree, the Young´s modulus is highly sensitive to the presence of defects as pores. The morphological analysis performed to reveal the spherulites evidenced the presence of porosity due to the pore peroxide removal (Figure 1). The percentage of porosity increased with the peroxide content, reaching values up to ~ 14% for the PP-CR546 (Table 5). Therefore, the elastic modulus evolves with the peroxide content just the opposite way as the porosity does.

Concerning the strength properties, the yield stress showed a slight decrease with a small addition of peroxide but seemed not to be influenced by the amount included. On the contrary, the stress and strain at break presented a significant change with the peroxide content. Both magnitudes tended to diminish as the amount of peroxide increased and this tendency is in accordance with the relationships between the mechanical properties and the molecular weight reported for reactor-made grades previously (Dasari et al., 2003a, 2003b, 2003c; Ogawa, 1992; Sugimoto et al., 1995). The reduction in the molecular weight with the peroxide content involves changes above all in the amorphous part and the results obtained for the tensile stress at break and the strain at break evidence that they are predominantly governed by this amorphous region. However, an exception is noted. The strain at break of CRPP154 diverted from this tendency and the value obtained was the highest. This observation was also shown by Azizi & Ghasemi, 2004, who assumed that at low levels of peroxide content the high molecular weight tail of PP matrix was degraded while the low molecular weight remained unchanged and therefore the slippage of polymer chains could be easier and greater.

	E (MPa)*	σ_{ys} (MPa)	σ_t (MPa)	ε_r (%)
PP0	1336	33.9 ± 0.3	20.4 ± 0.3	145 ± 50
PP-CR154	1231	31.5 ± 0.4	19.0 ± 0.5	320 ± 110
PP-CR402	1245	31.9 ± 0.3	17.5 ± 0.9	90 ± 60
PP-CR546	1241	31.1 ± 0.4	16 ± 2	44 ± 12

Table 6. Mechanical properties, such as the Young´s modulus, E, the yield stress, σ_{ys}, the tensile strength, σ_t, and the elongation at break, ε_r, of the propylene homopolymer, PP0, and the controlled-rheology polypropylenes, PP-CR154, PP-CR402 and PP-CR546.*The standard deviations of the Young´s modulus were not available.

5.4.2 Controlled-rheology EPBCs

The mechanical properties of the reactor-made copolymers, EPBC0 and EPBC0-2, and controlled-rheology EPBCs are presented in Table 7. Regarding the elastic properties, the Young´s modulus decreases with the peroxide content, which is not surprising since the cristallinity is reduced with the peroxide treatment (Table 4). As already discussed for the

polypropylenes, this phenomenon can be explained with the help of the degree of cristallinity. The elastic modulus is highly dependent on the stiffest part of the structure, that is, the crystalline region (Avella et al., 1993; Dasari et al., 2003a; Van der Wal et al., 1998); thus, the lower the latter, the lower the former.

The yield stress reduces with increasing peroxide content and this tendency is in accordance with the relationships between the mechanical properties and the molecular weight reported elsewhere (Ogawa, 1992; Dasari et al., 2003b; Van der Wal et al., 1999). However, in this case two exceptions are remarkably. Firstly, the elongation at break increases with the addition of DTBP up to 101 ppm concentration and decreases after that. This behaviour has been also shown for the polypropylenes (Table 6) and a possible explanation to this fact was given by Azizi & Ghasemi, 2004. It is assumed that at low levels of peroxide content the high molecular weight tail of PP matrix was degraded while the low molecular weight remained unchanged and therefore the slippage of polymer chains could be easier and greater. Secondly, the other parameter that shows an anomalous trend is the tensile strength, which initially decreased with the addition of peroxide but for greater amounts of DTBP, a sudden increase occurs. At this degree of copolymer degradation, probably the elastomeric phase could be constituted by either solid crosslinked particles or high molecular weight highly branched species and the failure properties were transferred to the minority phase (Berzin et al., 2001).

	E (MPa)	σ_{ys} (MPa)	σ_t (MPa)	ε_r (%)
EPBC0	1165 ± 20	25.2 ± 0.5	17.5 ± 0.5	92 ± 50
EPBC0-2*	1291	23.4	16.5	161
EPBC-CR101	1061 ± 15	23.9 ± 0.3	17.2 ± 0.3	175 ± 42
EPBC-CR332	1022 ± 31	22.6 ± 0.1	15.1 ± 0.5	49 ± 23
EPBC-CR471	995 ± 30	22.2 ± 0.1	17.5 ± 0.3	58 ± 4

Table 7. Mechanical properties, such as the Young´s modulus, E, the yield stress, σ_{ys}, the tensile strength, σ_t, and the elongation at break, ε_r, of the reactor-made copolymers, EPBC0 and EPBC0-2, and the controlled-rheology EPBCs, EPBC-CR101, EPBC-CR332 and EPBC-CR471. *The standard deviations of the mechanical properties of EPBC0-2 were not available.

With the aim of evaluating the influence of the reactive extrusion on the mechanical properties, the comparison of the mechanical properties between the reactor-made EPBC0-2 and the controlled-rheology EPBC-CR101 with similar structural properties draws some information. The elastic modulus of the reactor-made copolymer is higher than that of the peroxide degraded copolymer and this is in accordance with the crystallinity degree (Table 4). The percentage of crystallinity of the reactor-made copolymer is slightly higher than that of the controlled-rheology copolymer as in the former there are no crosslinkings in the elastomeric phase which lead to obstruct the crystalline architecture. In contrast, the yield stress, tensile strength and elongation at break of EPBC0-2 are a bit lower than those of the EPBC-CR101. The crosslinks produced in the elastomeric phase during the peroxide degradation give rise to copolymers with the capacity to absorb more energy than the reactor-made copolymer.

5.5 Fracture characterization

5.5.1 Fracture behavior of controlled-rheology PPs

Figure 3 shows the load (P) – load line displacement (δ) records obtained from fracture tests at room temperature and at quasi-static conditions (low loading rates) of propylene homopolymer, PP0, and thee controlled-rheology PPs. The mechanical response for all the materials presented clearly elastic-plastic behaviour and this justifies the use of the EPFM multiple specimen method to evaluate the fracture behaviour. In addition, all the curves deviated from linearity and at a certain deflection level, sudden instability occurred and the specimen broke in two halves. The difference in stiffness is due to the different initial crack lengths.

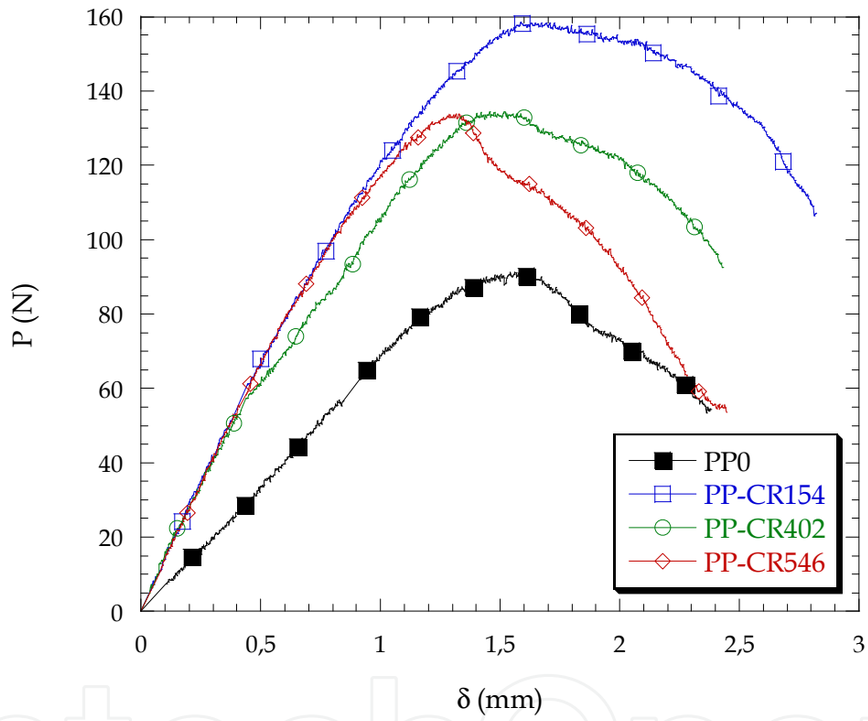

Fig. 3. Load (P) versus load-line displacement (δ) of the polypropylene homopolymer, PP0, and controlled-rheology polypropylenes, CRPP154, CRPP402 and CRPP546.

Figure 4 presents the J-R curves constructed for the propylene homopolymer, PP0, and the controlled-rheology PPs, PP-CR154, PP-CR402 and PP-CR546. These plots also include the fit of the J-crack growth resistance curve to the power law $J=C\cdot\Delta a^{N}$, with $N\leq 1$. The reactor-made polypropylene was the toughest material and the addition of peroxide acts in detriment of the toughness. This is indicated more clearly in Figure 5 where the crack growth initiation energy, J_{IC}, determined following the guidelines described by Hale & Ramsteiner, 2001, is plotted. All the fracture toughness values verified the size criterion described by equation 8, the fulfilment of which guarantees the plane strain state. As expected, the fracture toughness values drop abruptly with a small addition of peroxide and this decrease continues gradually with peroxide content.

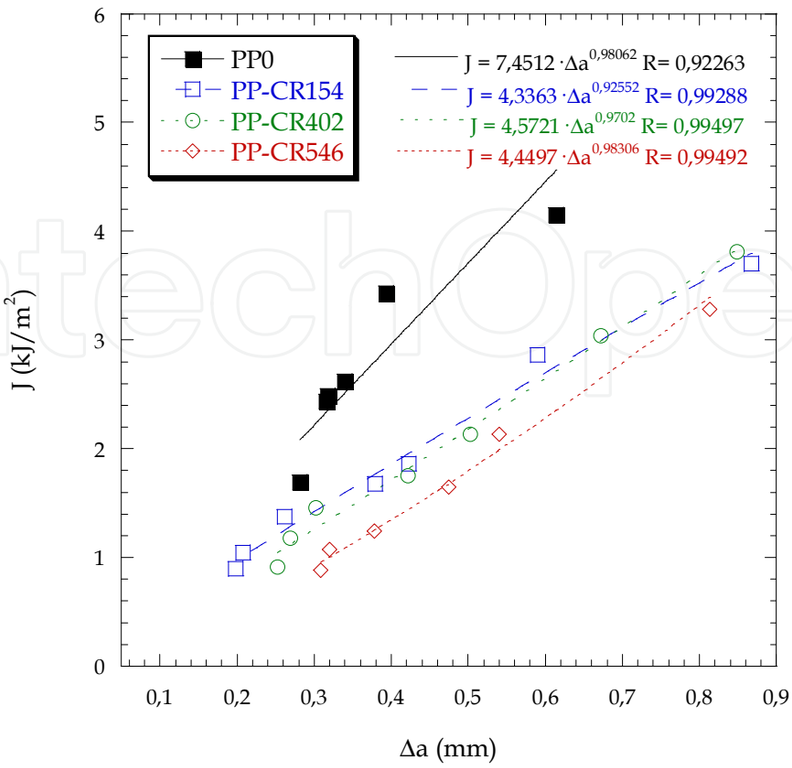

Fig. 4. J-R curves of polypropylene homopolymer, PP0, and controlled-rheology polypropylenes, PP-CR154, PP-CR402 and PP-CR546.

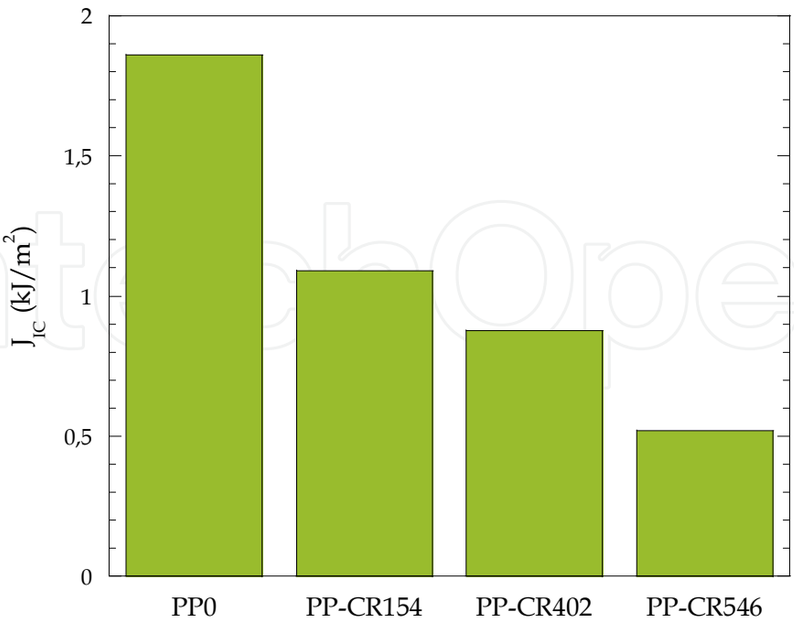

Fig. 5. Evolution of the crack growth energy, J_{IC}, with peroxide content of the polypropylenes under study.

The loss of ductility with the addition of peroxide can be easily observed in Figure 6, which shows the micrographs obtained via light microscopy and performed on the fracture surfaces of the tested specimens broken afterwards at liquid nitrogen and high loading rates to reveal the stable crack length. All the polypropylenes underwent stable crack length with ~ 0.3 mm in size. Independently of the material, three regions were distinguishable. The first one, close to the notch tip, is attributed to stable crack propagation. This zone is followed by a stress whitened area and ahead of it; the remainder of the fracture surface is characterized by a rough, un-whitened and uniform area related to the virgin material. Two main features can be drawn from the analysis of these fracture surfaces. Firstly, the stable crack length is more and more diffuse with the peroxide content. Indeed, to minimise the risk of incorrect measurements in the crack length, scanning electron microscopy means were to be used in the peroxide degraded polypropylenes instead of light microscopy. Secondly, the intensity and the extension of the stress- whitened region ahead of the stable crack length were

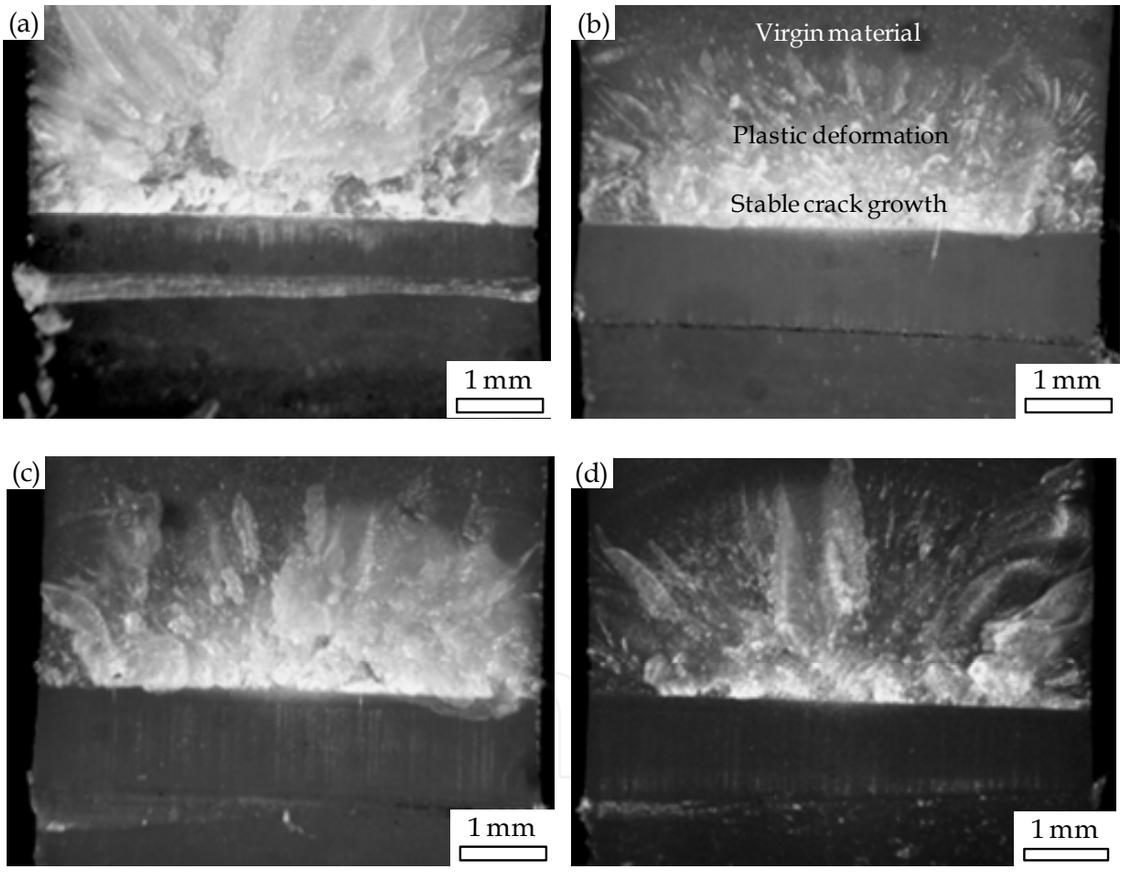

Fig. 6. Fracture surfaces obtained via light microscopy of (a) PP0, (b) PP-CR154, (c) PP-CR402 and (d) PP-CR546. All the specimens showed a stable crack length ~ 0.3 mm. By way of example, the three characteristic regions appearing in the fracture surfaces are indicated in CRPP154 micrograph.

reduced with the addition of peroxide. This very tendency has been also observed previously (Avella et al., 1993; Fukuhara, 1999; Sugimoto et al., 1995). They focused their research on understanding the effect of Mw on the fracture toughness of semicrystalline

polymers, and observed that the fracture toughness increased strongly with increasing molecular weight. The key factor were the tie molecules which join the lamellae bundles together. As the molecular weight lowers, the number of tie molecules decreases, the material becomes less interconnected and the fracture occurs at lower stress and strain levels.

Finally, the fractographic study revealed little differences among the four materials with different rheological properties (Figure 7). The analysis of the stable crack region close to the notch displayed spherulites interconnected by amorphous regions, being the interspherulitic links breakage the dominant mode of failure (Lapique et al., 2000). Consequently, this type of morphology indicates that crazes are the main micromechanism of deformation. Upon loading, spherulites are separated from one another and sustained by tie molecules, the density and strength of which are diminished with the peroxide content. With increasing loading, craze area spreads out and propagates within the interspherulitic and amorphous regions. The cracks are formed when these fibrillar bridges fail (Avella et al., 1993; Botsis et al., 1989; Chen et al., 2002; Dasari et al., 2003a, 2003b, 2003c; Ibdhadon, 1998; Ogawa, 1992; Sugimoto et al., 1995).

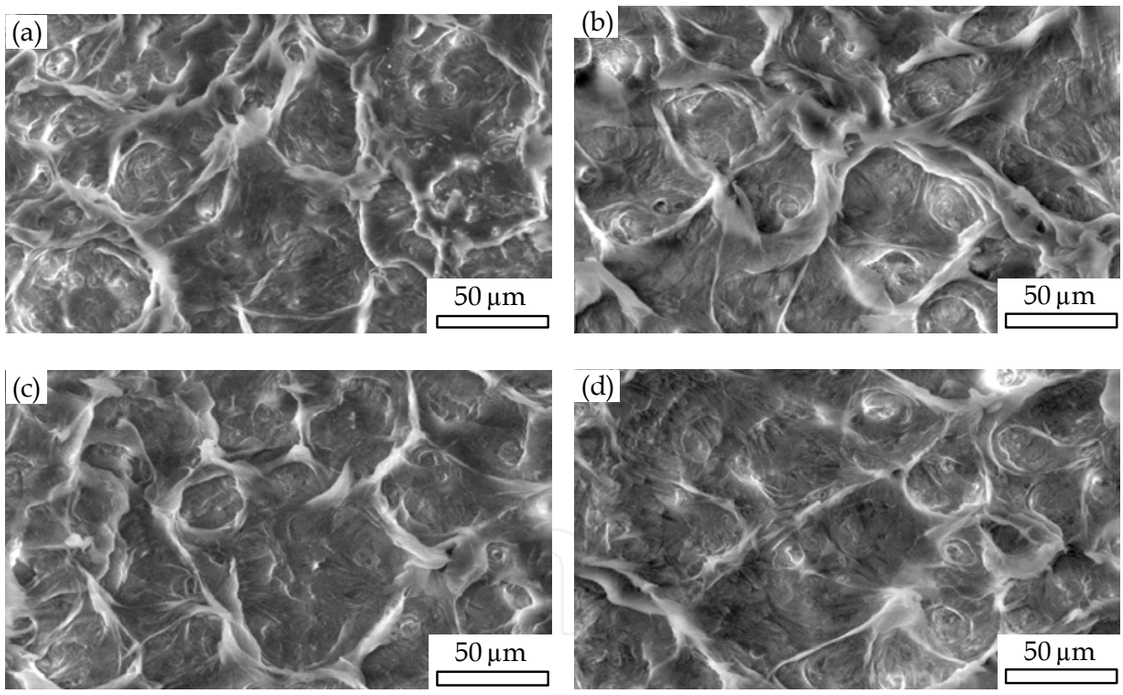

Fig. 7. Fracture surfaces obtained via scanning electron microscopy of the stable crack growth region close to the notch: (a) PP0, (b) CR-PP154, (c) CR-PP402 and (d) CR-PP546.

5.5.2 Fracture behavior of controlled-rheology EPBCs

Figure 8 presents the typical load (P) – load line displacement (δ) diagrams obtained from fracture tests at room temperature and at low loading rates for the reactor-made copolymer, EPBC0, and the controlled-rheology copolymers taking as the starting copolymer EPBC0, EPBC-CR101, EPBC-CR332 and EPBC-CR471. The mechanical response for all the

copolymers under study was clearly nonlinear with complete stable fracture. Therefore, the appropriate fracture mechanics procedure to characterize the fracture behaviour of these copolymers was the EPFM normalization method. Although all the materials showed not only the same geometry and size but also similar initial crack lengths, it is evident that the area under the curve, that is, the energy absorbed by the specimen, differs from that of the non-peroxide treated copolymer, EPBC0, to that with a small content of peroxide, EPBC-CR101, and even more to those with higher peroxide content as EPBC-CR332 and EPBC-CR471. The load relaxation, related to stable crack growth, occurred at lower load values as the peroxide content increases and the degree of fracture stability is also lesser prominent.

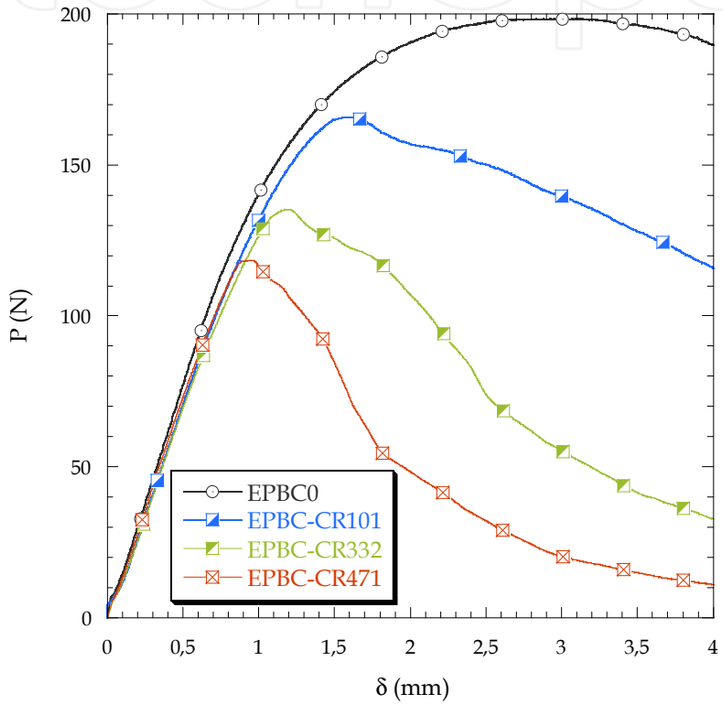

Fig. 8. Load (P) versus load-line displacement (δ) of the copolymer, EPBC0, and controlled-rheology copolymers, EPBC-CR101, EPBC-CR332 and EPBC-CR471

The J-R curves constructed for the non-degraded copolymer, EPBC0, and the peroxide-degraded copolymers, EPBC-CR101, EPBC-CR332 and EPBC-CR471, are shown in Figure 9. These plots also include the fit of the J-crack growth resistance curve to the power law $J=C\cdot\Delta a^{N}$, with $N\leq 1$. Analysis of the curves reveals that the reactor-made copolymer was the toughest material and the addition of peroxide acts in detriment of the toughness. Interestingly, the copolymers with the highest peroxide content, EPBC-CR332 and EPBC-CR471, showed almost flat resistance curves, indicating the remarkable loss of ductility with the peroxide content. This is clearly observed in Figure 10, where the crack initiation resistance, J_{IC}, of all the copolymers under study is presented. The fracture toughness of the peroxide-degraded copolymers verified the size requirement specified in equation 8, the fulfilment of which guarantees plane strain state, but the value of the reactor-made copolymer was not in plane strain state. Even so, the values are comparable as all the fracture specimens are of the same thickness. As expected, the fracture values drop abruptly

with a small addition of peroxide and this reduction continues gradually with the peroxide content. This behaviour is similar to that shown by polypropylene homopolymers (Figure 5) and can aso be explained in terms of the molecular weight. The fracture toughness increases strongly with increasing molecular weight due to the linking molecules that join the crystalline blocks together. As the molecular weight decreases, the number of linking molecules also decreases, the material becomes less interconnected and fracture occurs at lower stress and strain levels (Avella et al., 1993; Fukuhara, 1999; and Sugimoto et al., 1995).

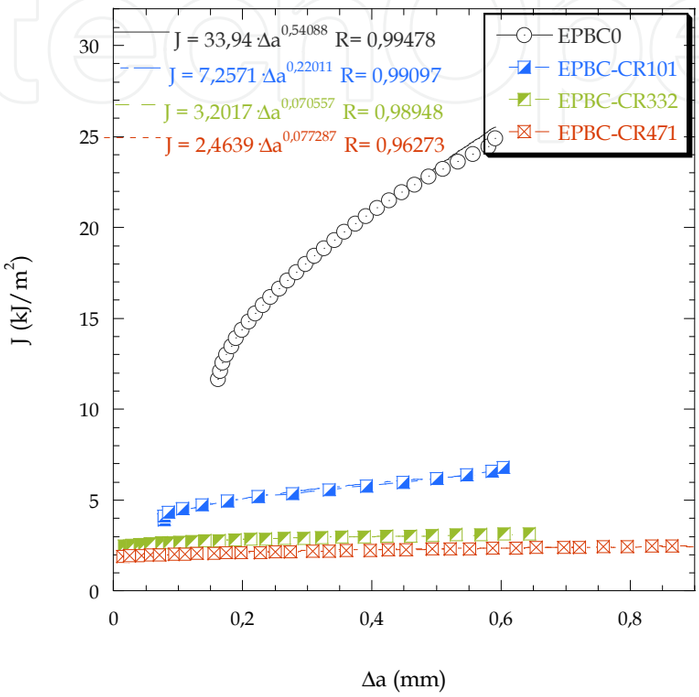

Fig. 9. J-R curves of the non-degraded copolymer, EPBC0, and the controlled-rheology copolymers, EPBC-CR101, EPBC-CR332 and EPBC-CR471.

The reduction of toughness and the loss of ductility with the addition of peroxide is easily observed in Figure 11, which shows the micrographs obtained via light microscopy and performed on the fracture surfaces of the tested specimens broken afterwards at liquid nitrogen and high loading rates to reveal the stable crack length. All the copolymers underwent stable crack length with ~ 0.6 mm in size. Independently of the material, three regions are distinguishable. The first one, close to the notch tip, is attributed to the stable crack propagation. This zone is followed by a stress whitening area and, ahead of it, the remainder of the fracture surface is characterized by a rough, un-whitened and uniform area related to the virgin material. Two main features can be drawn from the analysis of these fracture surfaces. Firstly, the stable crack length is more and more diffuse with the peroxide content. Indeed, to minimise the risk of incorrect measurements in the crack length, scanning electron microscopy means was used for the peroxide degraded copolymers instead of light microscopy. Secondly, the intensity and the extension of the stress whitening region ahead of the stable crack length reduced with the addition of peroxide. These two factors explain the decrease of the slope of the R-curves with the addition of peroxide (Figure 9).

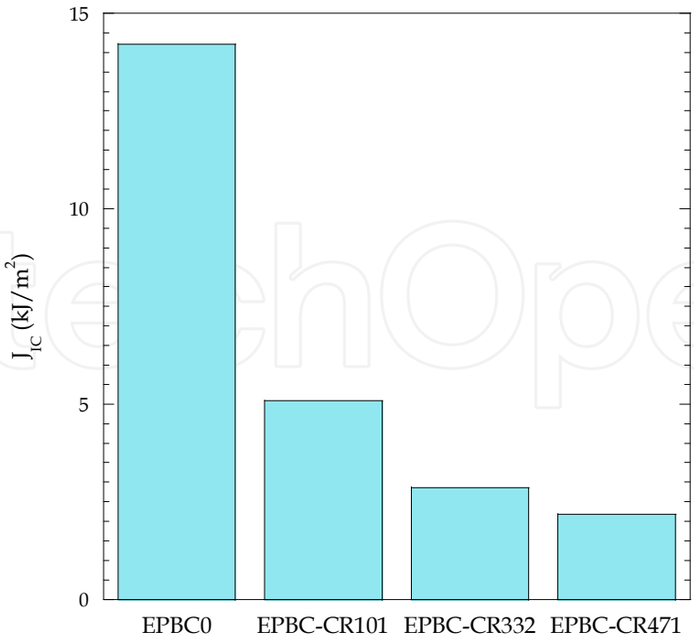

Fig. 10. Evolution of the crack growth energy, J_{IC}, with peroxide content of the copolymers under study.

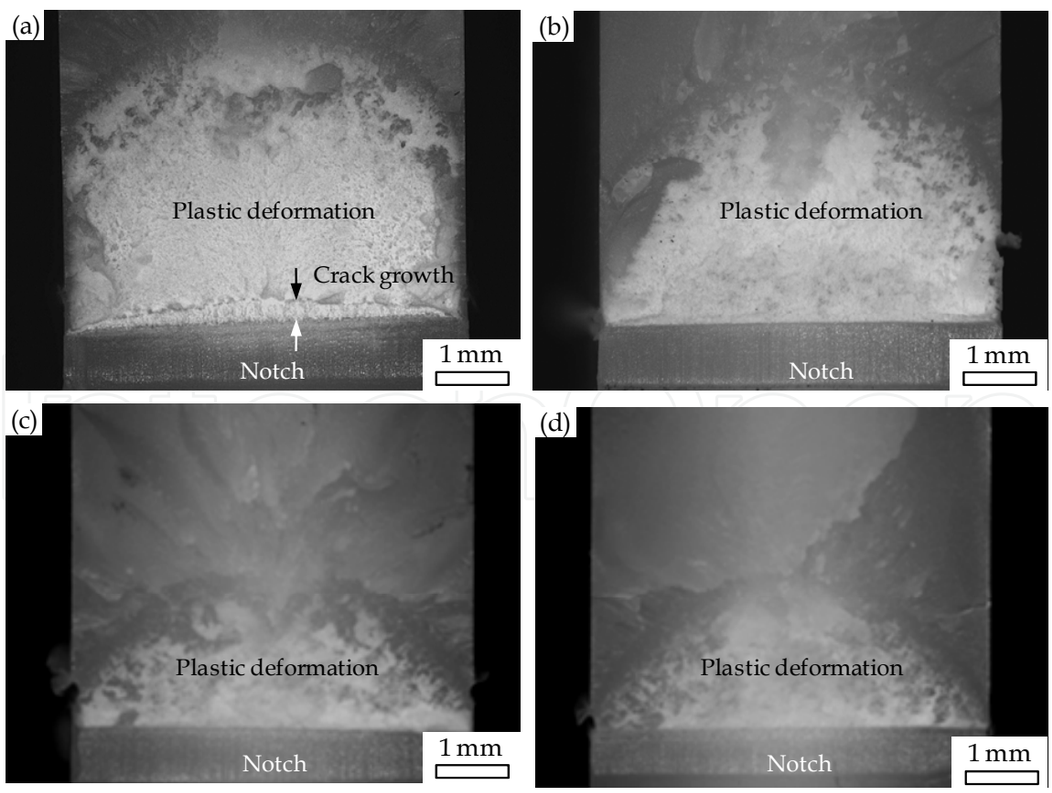

Fig. 11. Fracture surfaces obtained via light microscopy: (a) EPBC0, (b) EPBC-CR101, (c) EPBC-CR332 and (d) EPBC-CR471. All specimens show a stable crack length of ~ 0.6 mm.

The fracture surfaces were also examined via scanning electron microscopy with the aim of analyzing more deeply the fracture behaviour of controlled-rheology-copolymers. Figure 12 shows the morphology of the stable crack growth region for every copolymer. All the fracture surfaces displayed a macroductile tearing formed by broken stretched filaments oriented in the perpendicular direction to the crack propagation. Upon loading, small cavities were nucleated at the weak points of the copolymer such as the boundary between the elastomeric particles and the PP matrix or the intercrystalline zones in the PP matrix (Dasari et al.; 2003a; Doshev et al., 2005; Grellmann et al., 2001;. Starke et al., 1998; Yokoyama & Riccò, 1998). These voids were stabilised by fibrillar bridges of PP filaments which were plastically deformed and orientated. With consequent increase in deformation, excessive plastic flow occurred at these PP filaments and a stable crack nucleated and propagated through the closely PP bridges giving rise to the fibrillated morphology with ductile pulling of ligaments left behind. It is worth mentioning that the extension of such a ductile tearing was less pronounced with the addition of DTBP as the strength of these fibrillar PP bridges was reduced as the molecular weight lowered.

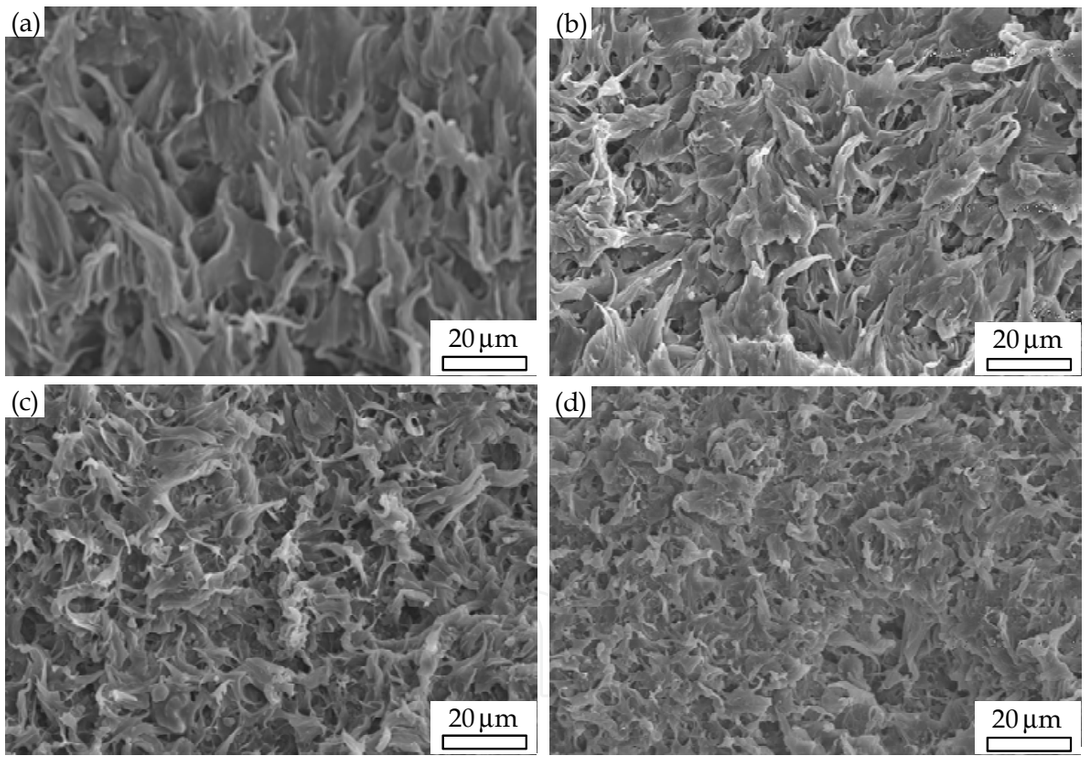

Fig. 12. Fracture surfaces obtained via scanning electron microscopy of the stable crack growth zone close to the notch: (a) EPBC0, (b) CR-EPBC101, (c) CR-EPBC332 and (d) CR-EPBC471.

The nucleation and growth of this mechanism of failure was clearly observed in the stress whitening region, which occurred ahead of the stable crack growth zone, of the post mortem fracture surfaces (Figure 13). The micrographs reveal the way the voids grow around the elastomeric phase. Despite the different content in peroxide, no appreciable differences could be evidenced in this region.

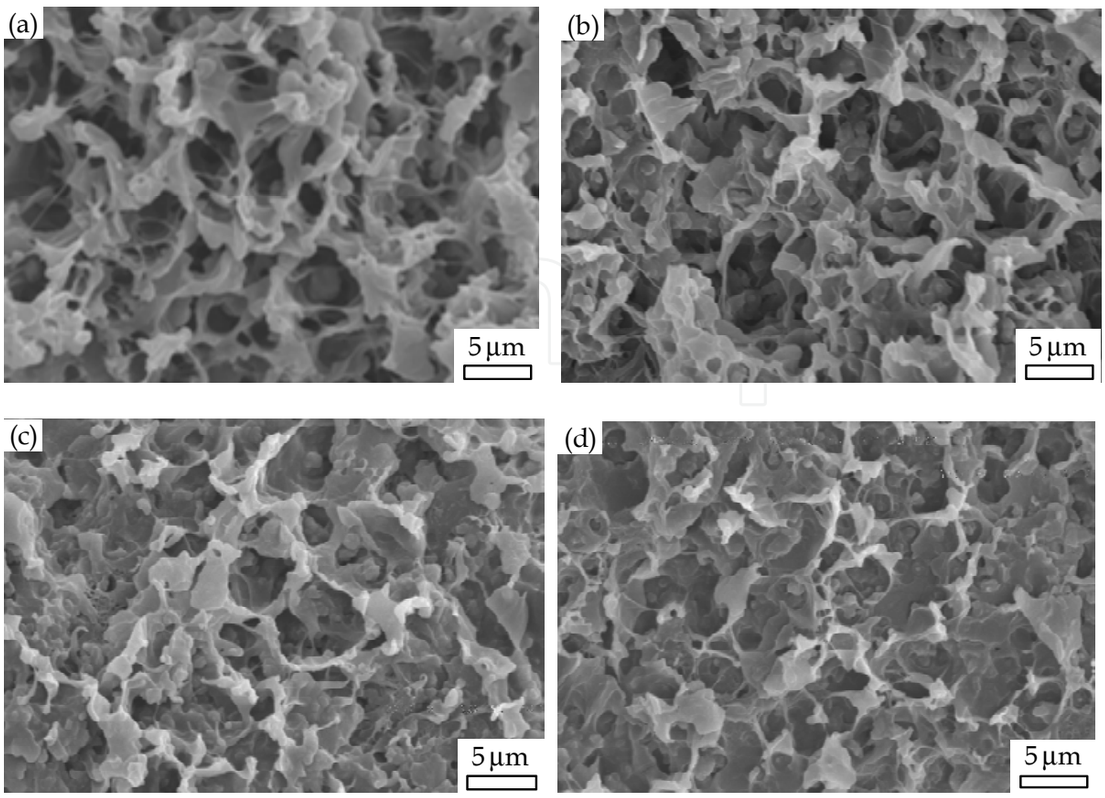

Fig. 13. Stress whitening region associated to plastic deformation ahead of the stable crack growth obtained from post-mortem fracture surfaces: (a) EPBC0, (b) CR-EPBC101, (c) CR-EPBC332 and (d) CR-EPBC471

5.6 Relationship between spherulite size and fracture toughness

The relationship between fracture toughness and molecular weight has been amply demonstrated in controlled-rheology polyproypylenes and copolymers in the preceding sections. Besides, it has been also shown that the decrease in the molecular weight is closely correlated with an increase in the spherulite diameters (Figures 1 and 2). Figure 14 represents the relationship between the fracture toughness and the spherulite size of the reactor-made polypropylene, PP0, and the controlled-rheology polypropylenes, PP-CR154, PP-CR402 and PP-CCR546. As observed, the fracture toughness is highly dependent not only on the molecular characteristics but also on supramolecular characteristics as the spherulites (Ibhadon, 1998): the bigger the spherulite diameter the lower the fracture toughness. The increase of the crystalline size declines the number and flexibility of the molecular chains which control the fracture toughness. The contribution to the fracture toughness is determined by the energy required to strain and break the tie molecules which hold together the lamellae bundles. Upon loading, the lamellae bundles separation is accompanied by massive voiding with the simultaneous onset of a craze like a microporous structure. As the molecular weight is decreased, the spherulite size is raised and hence, the density of tie molecules is suppressed impeding the formation of this microporous structure within the spherulitic and interspherulitic regions (Chen et al., 2002). This favours the

brittleness and therefore the reduction in the fracture toughness with the increase of the spherulite diameter/addition of peroxide content.

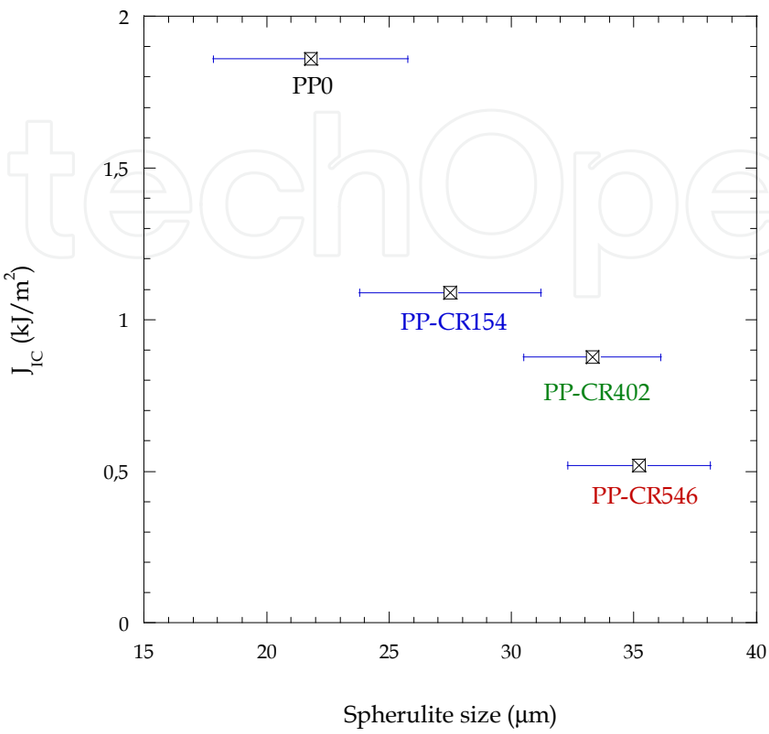

Fig. 14. Frature toughness, J_{IC}, versus the spherulite size of the reactor-made polypropylene, PP0, and the controlled-rheology polypropylenes, PP-CR154, PP-CR402 and PP-CR546.

It is worth mentioning that the controlled-rheology polypropylenes PP-CR402 and PP-CR546 are very similar from the structural (analogous molecular weight characteristics) (Table 1) and morphological (spherulite size) (Table 5) points of view. However, their fracture toughness values are quite different (Fig. 14). This disparity does not correlate properly with the small differences observed in the size of the spherulites but does with the variation in the porosity (Table 5). PP-CR546 presented a ~ 14% of porosity versus a ~ 8% for CRPP402.

5.7 Fracture behaviour of controlled-rheology versus conventional grades

Although the reactor-made copolymer EPBC0-2 presents analogous structural properties to the peroxide degraded copolymer EPBC-CR101 (molecular weights, MWD and melt flow rate) (Table 2), it has been shown some distinctness in both thermal and mechanical properties. In general, the thermal and mechanical properties of EPBC0-2 were more similar to the other reactor-made copolymer EPBC0 than to the controlled-rheology copolymer EPBC-CR101. With the aim of evaluating if fracture behaviour sustained this trend, Figure 15 shows the resistance curves of EPBC0-2 and EPBC-CR101 obtained at room temperature and low loading rates. These plots also include the fit of the J-crack growth resistance curve to the power law $J=C \cdot \Delta a^N$, with $N \leq 1$. Despite the likeness in the structural properties the J-R

curves are completely different. Moreover, the fitting parameters of EPBC0-2 are similar to those of the EPBC0 (Fig. 9). This is more clearly seen when comparing the crack growth initiation energy of these copolymers, which were 14.2, 14.0 and 5.09 kJ/m² for EPBC0, EPBC0-2 and EPBC-CR101, respectively. Both EPBC0 and EPBC0-2 were not in plane strain state as neither of them verified the size criterion displayed in equation 8.

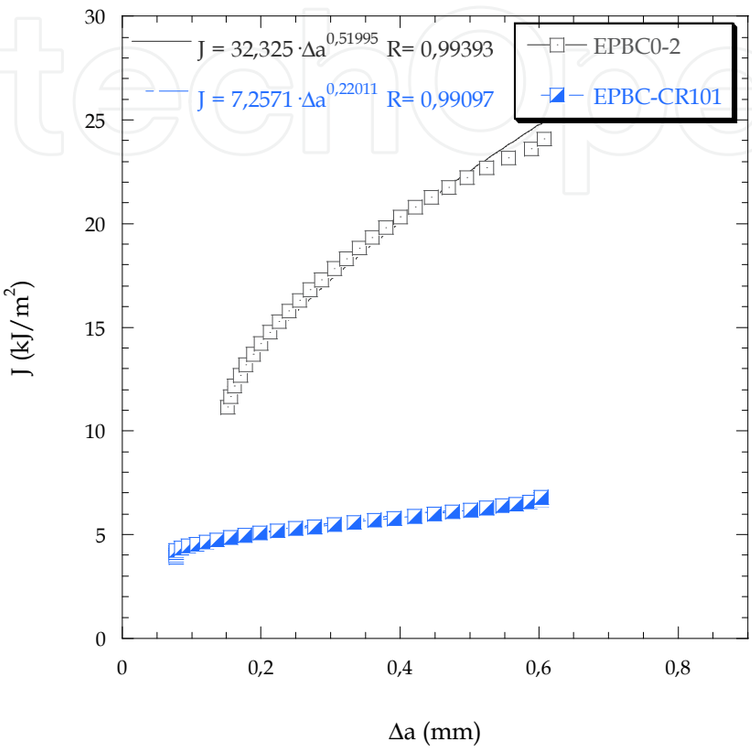

Fig. 15. J-R curves of a rector-made copolymer, EPBC0-2, and rheology controlled copolymer, EPBC-CR101, with similar structural characteristics (molecular weights and melt flow rate) (Table 5).

Interestingly, not only the measurements of J-fracture toughness values but also the fractographic analysis performed via optical microscopy indicated that the reactor-made EPBC0-2 copolymer was tougher than the reactive extrusion copolymer EPBC-CR101. Figure 16 shows the optical micrographs of the fracture surfaces broken after the test at liquid nitrogen temperature and high loading rates of EPBC0-2 and EPBC-CR101. The stable crack growth in both materials was ~ 0.6 mm. It is evident that the stable crack length is more easily distinguishable in EPBC0-2 than in EPBC-CR101. Besides, both the intensity and the extension of the stress-whitening region ahead of the stable crack growth are more pronounced in EPBC0-2 than in EPBC-CR101. Furthermore, when comparing the optical fracture surface of EPBC0 (Fig. 11a) with that of EPBC0-2 (Fig. 16a), scarce differences can be observed.

The fractographic analysis carried out via scanning electron microscopy on EPBC0-2 showed the same micromechanism of failure as that described for the controlled-rheology copolymers, that is, macroductile tearing formed by broken stretched filaments oriented in the direction perpendicular to the crack propagation (Fig. 17). However, the ductile tearing

of EPBC0-2 is more marked than that of EPBC-CR101. Once more, there is more similarity between the fracture surfaces of reactor-made copolymers, EPBC0 (Fig. 12a) and EPBC0-2 (Fig. 17a), than between the copolymers with analogous structural properties but processed by distinct procedures (Fig. 17).

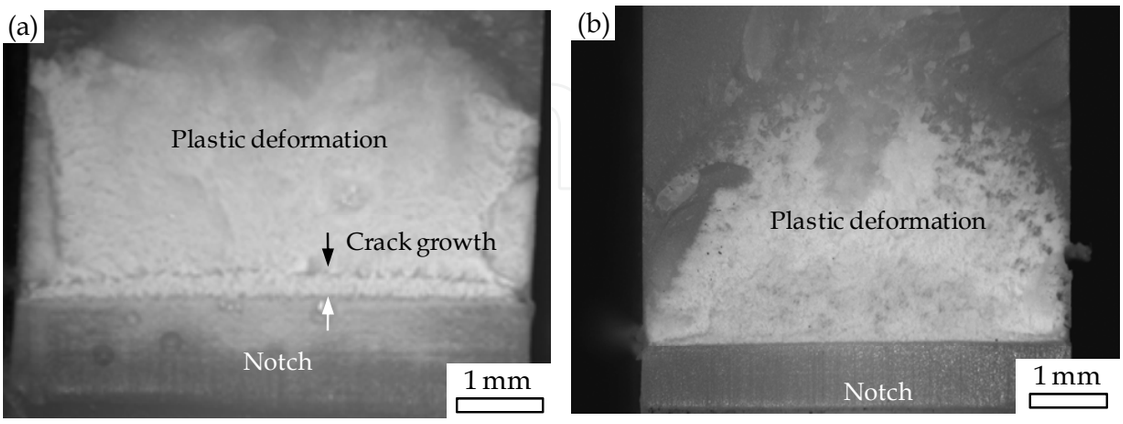

Fig. 16. Fracture surfaces obtained via light microscopy of (a) the reactor-made copolymer EPBC0-2 and (b) rheology controlled copolymer EPBC-CR101. Both materials are characterized by similar structural properties. The specimens presented a stable crack length of ~ 0.6 mm.

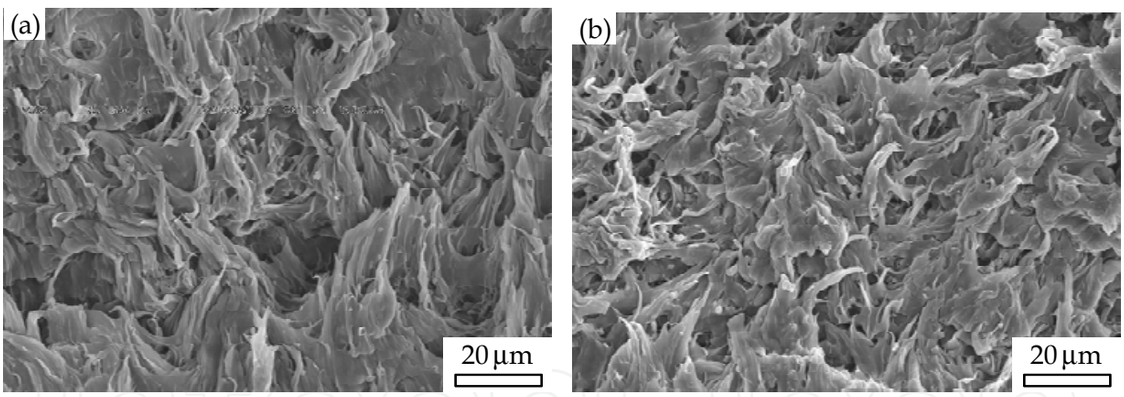

Fig. 17. Fracture surfaces obtained via scanning electron microscopy of (a) the reactor-made copolymer EPBC0-2 and (b) rheology controlled copolymer EPBC-CR101. Both materials are characterized by similar structural properties.

Finally, the reactor-made copolymer, EPBC0-2, results to be a very tough material with excellent mechanical properties and above all, superior processing properties, analogous to those of peroxide-degraded copolymers.

6. Conclusions

A set of controlled-rheology propylene homopolymers and ethylene-propylene block copolymers have been analyzed. The investigation has been focussed on the influence of the DTBP addition on the supramolecular characteristics as the spherulite size and distributuion

of these semicrystalline polypropylenes and above all, on the fracture behaviour under EPFM. Besides, an in-depth and systematic analysis of the MWD, thermal and mechanical properties has also been performed. Finally, controlled-rheology and conventional grades with similar structural properties were compared to evaluate the goals and limitations of the reactive extrusion process. The main conclusions of each of these aspects are:

- For either the propylene homopolymer or copolymers, the peroxide reduced the molecular weight and narrowed the MWD leading to an increase of the MFR. This reduction was more pronounced in the propylene homopolymers than in the copolymers because in the latter, two competing effects were present: β-scissions of the long PP chains and chain branching and crosslinking of the PE phase.
- Concerning the thermal properties, the melting temperature reduced with the peroxide content for both the propylene homopolymers and the copolymers. However, the crystalline degree remained constant with the peroxide addition for the propylene homopolymers but reduced slightly for the copolymers. The crosslinks produced in the elastomeric phase may disturb the crystallinity architecture of the copolymers.
- Regarding the evolution of the supramolecular properties of the propylenes homopolymers, the average spherulite size seems to enhance and the distribution width seems to reduce, attaing a more unifrom distribution, as the DTBP content increases. The reduction of M_w, promoted by peroxide addition, leads to the maintenace of the crystalline degree, with the only growth of the spherulite size at the expense of the reduction in the density of tie molecules. However, for very high peroxide content, this trend is not followed because of the presence of pores.
- In general, the mechanical properties tends to decrease with the peroxide content. The strength parameters as the yield stress, tensile strenght and elongation at break, are highly dependent on the molecular weight. The increase in peroxide content entails a decrease in the molecular weight which preferentailly affects the amorphous regions. However, some exceptions were observed in the evolution of the tensile strength and elongation at break with the peroxide addition of the copolymers. This anomalous behavious can be also explained in the light of the presence of the long residual chains of PE which were probably branched.
- Concerning the fracture behaviour, the fracture toughness values of either the reactor-made polypropylenes or copolymers were the highest of all the materials under study. Independently of the material, the fracture toughness dropped abruptly with a small addition of peroxide content and a continuous reduction with further addition of DTBP. In addition, the copolymer experienced an appreciable loss of ductility with the peroxide content not only evident form the load-displacement records and the naked-eye examination ofo the fracture surfaces but also from the slope of the J-R curves.
- In case of PPs, the mechanism of failure of all the materials was crazing and no differences were found in the fracture surfaces among the different grades of polypropylene. All the results point at the influence of molecular weight which is closely related to the amorphous region. On the other hand, the mechanism of failure of all the copolymers analyzed involved growth of voidds around the elastomeric particles which resulted in a macroductile tearing. The degree of ductile tearing was less marked as the polymer degradation was more accentuated. Therefore, the reduction of the fracture parameters with the decrease in the molecular weight in semi-crystaline

propylene homopolymers and copolymers can be explained by the reduction in number and strength of the linking molecules that join the crystalline blocks.

- Finally, the controlled-rheology and the reactor-made EPBCs with similar structural characteristics presented diferences in the mechanical properties, being specially remarkable in the fracture behaviour. The micromechanisms of failure of both types of copolymers were similar although more likeness was found between the fracture surfaces of the reactor-made copolymers than between the copolymers with analogous structural parameters processed by distinct procedures.

7. Acknowledgment

The author is indebted to Ministerio de Educación of Spain for its financial support through project MAT2009-14294 and to REPSOL for the materials supply.

8. References

Allen, G. & Bevington, J.C. (1989). *Comprehensive Polymer Science. The synthesis, characterization, reactions and applications of polymers; Vol. 2 Mechanical properties*. Colin booth & Colin Price Eds. Pergamon Press, ISBN 0080325157, Oxford, UK

Asteasuain, M.; Sarmoria, C. & Brandolin, A. (2003). Controlled rheology of polypropylene: modelling of molecular weight distributions. *Journal of Applied Polymer Science*, Vol.88, No.7, (May 2003), pp. 1676-1685, ISSN 1097-4628

Avella, M.; dell´Erba, R.; Martuscelli, E. & Ragosta, G. (1993). Influence of molecular mass, thermal treatment and nucleating agent on structure and fracture toughness of isotactic polypropylene. *Polymer*, Vol.34, No.14, (1993), pp. 2951-2960, ISSN 0032-3861

Azizi, H. & Ghasemi, I. (2004). Reactive extrusion of polypropylene: production of controlled-rheology polypropylene (CRPP) by peroxide-promoted degradation. *Polymer Testing*, Vol.23, No.2, (April 2004), pp. 137-143, ISSN 0142-9418

Azizi, H.; Ghamesi, I. & Karrabi, M. (2008). Controlled-peroxide degradation of polypropylene: rheological properties and prediction of MWD from rheological data. *Polymer Testing*, Vol.27, No.5, (August 2008), pp. 548-554, ISSN 0142-9418

Baik, J.J. & Tzoganakis, C. (1998). A study of extrudate distorsion in controlled-rheology polypropylenes. *Polymer Engineering and Science*, Vol.38, No.2, (February 1998), pp: 274-281, ISSN 1548-2634

Baldi, F. & Riccò, T (2005). High rate J-testing of toughened polyamide 6/6: applicability of the load separation criterion and the normalization method. *Engineering Fracture Mechanics,* Vol.72, No.14, (September 2005), pp. 2218–2231, ISSN 0013-7944

Barakos, G.; Mitsoulis, E.; Tzoganakis, C. & Kajiwara, T. (1996). Rheological characterization of controlled-rheology polypropylenes using integral constitutive equation. *Jourrnal of Applied Polymer Science*, Vol.59, No.3, (January 1996), pp. 543-556, ISSN 1097-4628

Bernal, C.R.; Montemartini, P.E. & Frontini P.M. (1996) The use of load separation criterion and normalization method in ductile fracture characterization of thermoplastic polymers. *Journal of Polymer Science Part B - Polymer Physics*, Vol.34, No.11, (August 1996), pp. 1869–1880, ISSN 0887-6266

Berzin, F.; Vergnes, B. & Delamare L. (2001). Rheological behaviour of controlled-rheology polypropylenes by peroxide-promoted degradation during extrusion: comparison

between homopolymer and copolymer. *Journal of Applied Polymer Science*, Vol.80, No.8, (May 2001), pp. 1243-1252, ISSN 1097-4628

Blancas, C. & Vargas, L. (2001). Modeling of the industrial process of peroxide initiated polypropylene (homopolymers) controlled degradation. *Journal of Macromolecular Science Part B-Physics,* Vol.40, No.3-4, (2001), pp. 315-326, ISSN 0022-2348

Botsis, J.; Oerter, G. & Friedrich, K. (1999). Fatigue fracture in polypropylene with different spherulitic sizes. In: *Imaging and image analysis application for plastics*, B. Pourdeyhimi, (Ed.), 289-298, ISBN 978-1-884207-81-5, North Carolina State University, NC, USA

Braun, D.; Richter, S.; Hellmann, G.P. & Rätzsch, M. (1998). Peroxy-initiated chain degradation, crosslinking and grafting in PP-PE blends. *Journal of Applied Polymer Science*, Vol.68, No.12, (June 1998), pp. 2019-2028, ISSN 1097-4628

Chen, H.B.; Karger-Kocsis, J.; Wu, J.S. & Varga, J. (2002). Fracture toughness of α- and β-phase polypropylene homopolymers and random- and block-copolymers. *Polymer,* Vol.43, No.24, (November 2002), pp. 6505-6514, ISSN 0032-3861

Dasari, A.; Rohrmann, J. & Misra R.D.K. (2003). Microstructural evolution during tensile deformation of polypropylenes. *Materials Science and Engineering A*, Vol.351, (June 2003), pp. 200-213, ISSN 0921-5093

Dasari, A.; Rohrmann, J. & Misra R.D.K. (2003). Microstructural aspects of surface deformation processes and fracture of tensile strained high isotactic polypropylene. *Materials Science and Engineering A*, Vol.358, (October 2003), pp. 372-383, ISSN 0921-5093

Dasari, A.; Rohrmann, J. & Misra R.D.K. (2003). Surface microstructural modification and fracture behavior of tensile deformed polypropylene with different percentage crystallinity. *Materials Science and Engineering A*, Vol.360, (November 2003), pp. 237-248, ISSN 0921-5093

Do, I.H.; Yoon, L.K.; Kim, B.K. & Jeong, H.M. (1996). Effect of viscosity ratio and peroxide/coagent treatment in PP/EPR/PE ternary blends. *European Polymer Journal,* Vol.32, No.12, (December 1996), pp. 1387-1393, ISSN 0014-3057

Doshev, P.; Lach, R.; Lohse, G.; Heuvelsland, A.; Grellmann, W. & Radusch, H.J. (2005). Fracture characteristics and deformation behavior of heterophasic ethylene-propylene copolymers as a function of the dispersed phase composition. *Polymer*, Vol.46, No.22, (October 2005), pp. 9411-9422, ISSN 0032-3861

Ernst H.A.; Paris, P.C. & Landes J.D. (1981). Estimations on J-integral and Tearing Modulus T from a single specimen test record. *Fracture Mechanics: Thirteenth Conference ASTM STP 743*, Roberts R., (Ed.), pp. 476–502.

Fukuhara, N. (1999). Influence of molecular weight on J-integral testing of polypropylene. *Polymer Testing*, Vol.18, No.2, (April 1999), pp. 135-149, ISSN 0142-9418

Gahleitner, M.; Bernreitner, K.; Neiβl, W.; Paulik, C. & Ratajski. (1995). Influence of molecular structure on crystallization behavior and mechanical properties of polypropylene. *Polymer Testing,* Vol.14, No.2, (1995), pp. 173-187, ISSN 0142-9418

Gahleitner, M.; Wolfschwenger, J.; Bachner, C; Bernreitner, K. & Neiβl, K. (1996). Crystallinity and mechanical properties of PP-homopolymers as influenced by molecular structure and nucleation. *Journal of Applied Polymer Science*, Vol.61, No.4, (July 1996), pp. 649-657, ISSN 1097-4628

Graebling, D.; Lambla, M. & Wautier, H. (1997). PP/PE blends by reactive extrusion: PP rheological behavior changes. *Journal of Applied Polymer Science*, Vol.66, No.5, (October 1997), pp. 809-819, ISSN 1097-4628

Grein, C.; Plummer, C.J.G.; Kausch, H.H.; Germain, Y. & Béguelin, Ph. (2002). Influence of β nucleation on the mechanical properties of isotactic polypropylene and rubber modified isotactic polypropylene. *Polymer*, Vol.43, No.11, (May 2002), pp. 3279-3293, ISSN 0032-3861

Grellmann, W.; Seidler, S.; Jung, K. & Kotter, I. (2001). Crack-resistance behavior of polypropylene copolymers. *Journal of Applied Polymer Science*, Vol.79, No.13, (January 2001), pp. 2317-2325, ISSN 1097-4628

Hale, G.E. & Ramsteiner, F. (2001). J-fracture toughness of polymers at slow speed. In: *Fracture mechanics testing methods for polymers, adhesives and composites*, Moore, D.R.; Pavan, A. & Williams J.G., editors, pp 123-157, Elsevier Science Ltd. and ESIS, ISBN 0 08 043689 7, The Netherlands.

Hodgkinson, J.M.; Savadori, A. & Williams, J.G. (1983). A fracture mechanics analysis of polypropylene/rubber blends. *Journal of Materials Science*, Vol.18, No.8, (1983), pp. 2319-2336, ISSN 1573-4803

Ibhadon, A.O. (1998). Fracture mechanics of polypropylene: effect of molecular characteristics, crystallization conditions, and annealing on morphology and impact performance. *Journal of Applied Polymer Science,* Vol.69, No.13, (September 1998), pp. 2657-2661, ISSN 1097-4628

Karger-Kocsis, J. (1995). *Polypropylene: structures, blends and composites: copolymers and blends*. Chapman and Hall, ISBN 0-412-61420-0, London, UK

Kim, G.M.; Michler, G.H.; Gahleitner, M. & Fiebig, J. (1996). Relationship between morphology and micromechanical toughening mechanisms in modified polypropylenes. *Journal of Applier Polymer Science*, Vol.60, No.9, (May 1996), pp. 1391-1403, ISSN 1097-4628

Landes, J.D. & Begley, J.A. (1974). The results from J-integral studies: an attempt to establish a J_{IC} testing procedure. *Fracture Analysis, ASTM STP 560,* American Society for Testing and Materals, pp. 170-186.

Landes, J.D. & Zhou, Z. (1993). Application of load separation and normalization methods for polycarbonate materials. *International Journal of Fracture*, Vol. 63, No.4, (1993), pp. 383–393, ISSN 0376-9429

Lapique, F.; Meakin, P.; Feder, J. & Jossang, T. (2000). Relationships between microstructure, fracture-surface morphology, and mechanical properties in ethylene and propylene polymers and copolymers. *Journal of Applied Polymer Science*, Vol.77, No.11, (September 2000), pp. 2370-2382, ISSN 1097-4628

Morhain, C. & Velasco J.I. (2001). Determination of J-R curve of polypropylene copolymers using the normalization method. *Journal of Materials Science*, Vol.36, No.6, (March 2001) pp. 1487–1499, ISSN 1573-4803

Ogawa, T. (1992). Effects of molecular weight on mechanical properties of polypropylene. *Journal of Applied Polymer Science*, Vol.44, No.10, (April 1992), pp. 1869-1871, ISSN 1097-4628

Pabedinkas, A.; Cluett, W.R. & Balke, S.T. (1989). Process control for polypropylene degradation during reactive extrusion. *Polymer Engineering and Science,* Vol.29, No.15, (August 1989), pp. 993-1003, ISSN 1548-2634

Pasquini, N. (Ed.) (2005). *Polypropylene Handbook*. Hanser Publishers, ISBN 3-446-22978-7, Munich, Germany

Prabhat, K. & Donovan, J.A. (1985). Tearing instability in polypropylene. *Polymer*, Vol.26, No.13, (December 1985), pp. 1963-1970, ISSN 0032-3861

Rodríguez, C.; Maspoch, M.Ll. & Belzunce F.J. (2009). Fracture characterization of ductile polymers through methods based on load separation. *Polymer Testing,* Vol.28, No.2, (April 2009), pp. 204–208, ISSN 0142-9418

Ryu, S.H.; Cogos, C.G. & Xanthos, M. (1991). Parameters affecting process efficiency of peroxide-initiated controlled degradation of polypropylene. *Advances in Polymer Technology,* Vol.11, No.2, (July 1991), pp. 121-131, ISSN 1098-2329

Ryu, S.H.; Cogos, C.G. & Xanthos, M. (1991). Crystallization behavior of peroxide modified polypropylene. *Society of the Plastics Industry Annual Technical Conference ANTEC 1991*, pp. 886-888, Montreal, Canada

Salazar, A. & Rodríguez, J. (2008). The use of load separation parameter S_{pb} method to determine the J-R curves of polypropylenes. *Polymer Testing*, Vol.27, No.8, (December 2008), pp. 977–984, ISSN 0142-9418

Salazar, A.; Rodríguez, J.; Segovia, A. & Martínez, A.B. (2010). Influence of the notch sharpening technique on the fracture toughness of bulk ethylene-propylene block copolymers. *Polymer Testing*, Vol.29, No.1, (February 2010), pp. 49-59, ISSN 0142-9418

Salazar, A.; Rodríguez, J;. Segovia, A. & Martínez A.B. (2010). Relevance of the femtolaser notch sharpening to the fracture of ethylene-propylene block copolymers. *European Polymer Journal*, Vol.46, No.9, (June 2010), pp. 1896-1907, ISSN 0014-3057

Salazar, A.; Segovia, A.; Martínez, A.B. & Rodríguez, J. (2010). The role of notching damage on the fracture parameters of ethylene-propylene block copolymers. *Polymer Testing*, Vol.29, No.7, (October 2010), pp. 824-831, ISSN 0142-9418

Sheng, B.R.; Li, B.; Xie, B.H.; Yang, W.; Feng, J.M. & Yang, M.B. (2008). Influences of molecular weight and crystalline structure on fracture behaviour of controlled-rheology-propylene prepared by reactive extrusion. *Polymer Degradation and Stability*, Vol.93, No.1, (January 2008), pp. 225-232, ISSN

Sheskin, D.J. (2007). *Handbook of parametric and nonparametric statistical procedures*. 4th edition Chapman & Hall/CRC, ISBN 9781584888147, Florida (USA)

Starke, J.U.; Michler, G.H.; Grellmann, W.; Seidler, S.; Gahleitner, M.; Fiebig, J. & Nezbedova, E. (1998). Fracture toughness of polypropylene copolymers: influence of interparticle distance and temperature. *Polymer,* Vol.39, No.1, (January 1998), pp. 75-82, ISSN 0032-3861

Sugimoto, M.; Ishikawa, M. & Hatada, K. (1995). Toughness of polypropylene. *Polymer*, Vol.36, No.19, (1995), pp. 3675-3682, ISSN 0032-3861

Sun, Z. & Yu, F. (1991). SEM study on fracture behaviour of ethylene/propylene block copolymers and their blends. *Macromolecular Chemistry and Physics*, Vol.192, No.6, (June 1991), pp. 1439-1445, ISSN 1022-1352

Sun, Z.; Yu, F. & Qi, Y. (1991). Characterization, morphology and thermal properties of ethylene-propylene block copolymers, *Polymer*, Vol.32, No.6, (1991), pp. 1059-1064, ISSN 0032-3861

Teh, J.W.; Rudin, A. & Keung, J.C. (1994). A review of polyethylene–polypropylene blends and their compatibilization. *Advances in Polymer Technology*, Vol.13, No.1, (April 1994), pp. 1-23, ISSN 1098-2329

Thomann, R.; Wang, C.; Kressler, J.; Jüngling, S. & Mülhaupt, R. (1995). Morphology of syndiotactic polypropylene. *Polymer,* Vol.36, No.20, (1995), pp. 3795-3801, ISSN 0032-3861

Tjong, S.C.; Shen, J.S. & Li, R.K.Y. (1995). Impact fracture toughness of β-polypropylene. *Scripta Materialia,* Vol.33, (1995), pp. 503-508, ISSN 1359-6462

Tzoganakis, C.; Vlachopoulos, J.; Hamielec, A.E. & Shinozaki, D.M. (1989). Effect of molecular weight distribution on the rheological and mechanical properties of polypropylene. *Polymer Engineering and Science,* Vol.29, No.6, (March 1989), pp. 390-396, ISSN 1548-2634

Van der Wal, A.; Mulder, J.J. & Gaymans, R.J. (1998). Fracture of polypropylene: 2. The effect of crystallinity. *Polymer,* Vol.39, No.22, (October 1998), pp. 5477-5481, ISSN 0032-3861

Van der Wal, A.; Nijhof, R. & Gaymans R.J. (1999). Polypropylene–rubber blends: 2. The effect of the rubber content on the deformation and impact behavior. *Polymer*, Vol.40, No.22, (October 1999), pp. 6031-6044, ISSN 0032-3861

Varadarajan, R.; Dapp, E.K. & Rimnac C.M. (2008). Static fracture resistance of ultra high molecular weight polyethylene using the single specimen normalization method. *Polymer Testing*, Vol.27, No.2, (April 2008), pp. 260–268, ISSN 0142-9418

Wang, S.H.; Yang, W.; Xu, Y.J., Xie, B.H.; Yang, M.B. & Peng, X.F. (2008). Crystalline morphology of β-nucleated controlled-rheology polypropylene. *Polymer Testing*, Vol.27, No.5, (August 2008), pp. 638-644, ISSN 0142-9418

Wainstein, J.; Fasce, L.A.; Cassanelli, A. & Frontini P.M. (2007). High rate toughness of ductile polymers. *Engineering Fracture Mechanics*, Vol.74, No.13, (September 2007), pp. 2070–2083, ISSN 0013-7944

Wei, G.X.; Sue, H.J.; Chu, J.; Huang, C. & Gong, K. (2000). Toughening and strengthening of polypropylene using the rigid–rigid polymer toughening concept. Part I. Morphology and mechanical property investigations. *Polymer,* Vol.41, No.8, (April 2000), pp. 2947-2960, ISSN 0032-3861

Williams, J.G. (2001). Introduction to elastic-plastic fracture mechanics. In: *Fracture mechanics testing methods for polymers, adhesives and composites*, Moore, D.R.; Pavan, A. & Williams J.G., (Eds.), pp 119-122, Elsevier Science Ltd. and ESIS, ISBN 0 08 043689 7, The Netherlands.

Xu, T.; Yu, J. & Jin, Z. (2001). Effects of crystalline morphology on the impact behavior of polypropylene. *Materials & Design*, Vol.22, No.1, (February 2001), pp. 27-31, ISSN 0261-3069

Xu, T.; Lei, H. & Xie, C. (2002). The research on aggregation structure of PP materials under different condition and the influence on mechanical properties. *Materials & Design*, Vol.23, No.8, (December 2002), pp. 709-715, ISSN 0261-3069

Yokoyama, Y. & Riccò T. (1998). Toughening of polypropylene by different elastomeric systems. *Polymer*, Vol.39, No.16, (June 1998), pp. 3675-3681, ISSN 0032-3861

Yu, D.W.; Xanthos, M. & Gogos, C.G. (1990). Peroxide modified polyolefin blends: Part I. Effects on ldpe/pp blends with components of similar initial viscosities. *Advances in Polymer Technology*, Vol.10, No.3, (October 1990), pp. 163-172, ISNN 1098-2329

Yu, J.; Xu, T.; Tian, Y. Chen, X. & Luo, Z. (2002). The effects of the aggregation structure parameters on impact-fractured surface fractal dimension and strain-energy release rate for polypropylene. *Materials & Design*, Vol.23, No.1, (February 2002), pp. 89-95, ISSN 0261-3069

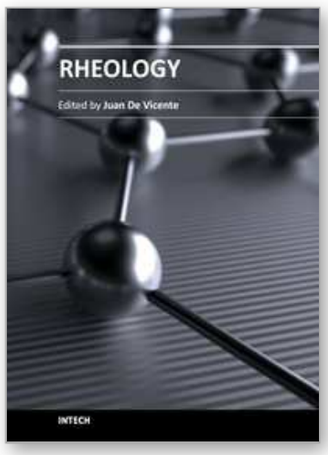

Rheology

Edited by Dr. Juan De Vicente

ISBN 978-953-51-0187-1
Hard cover, 350 pages
Publisher InTech
Published online 07, March, 2012
Published in print edition March, 2012

This book contains a wealth of useful information on current rheology research. By covering a broad variety of rheology-related topics, this e-book is addressed to a wide spectrum of academic and applied researchers and scientists but it could also prove useful to industry specialists. The subject areas include, polymer gels, food rheology, drilling fluids and liquid crystals among others.

How to reference

In order to correctly reference this scholarly work, feel free to copy and paste the following:

Alicia Salazar and Jesús Rodríguez (2012). Fracture Behaviour of Controlled-Rheology Polypropylenes, Rheology, Dr. Juan De Vicente (Ed.), ISBN: 978-953-51-0187-1, InTech, Available from: http://www.intechopen.com/books/rheology/fracture-behaviour-of-controlled-rheology-polypropylenes-

INTECH
open science | open minds

InTech Europe
University Campus STeP Ri
Slavka Krautzeka 83/A
51000 Rijeka, Croatia
Phone: +385 (51) 770 447
Fax: +385 (51) 686 166
www.intechopen.com

InTech China
Unit 405, Office Block, Hotel Equatorial Shanghai
No.65, Yan An Road (West), Shanghai, 200040, China
中国上海市延安西路65号上海国际贵都大饭店办公楼405单元
Phone: +86-21-62489820
Fax: +86-21-62489821

IntechOpen